

LASER DEBONDING OF CERAMIC ORTHODONTIC BRACKETS

Thesis submitted to the  
Faculty of Graduate Studies  
in partial fulfilment of the  
requirements for the degree of  
Master of Science

The University of Manitoba  
Department of Preventive Dental Science  
Winnipeg, Manitoba  
Canada

By  
Robert Maurizio Tocchio BSc., D.D.S.

April 26, 1990



National Library  
of Canada

Bibliothèque nationale  
du Canada

Canadian Theses Service    Service des thèses canadiennes

Ottawa, Canada  
K1A 0N4

The author has granted an irrevocable non-exclusive licence allowing the National Library of Canada to reproduce, loan, distribute or sell copies of his/her thesis by any means and in any form or format, making this thesis available to interested persons.

The author retains ownership of the copyright in his/her thesis. Neither the thesis nor substantial extracts from it may be printed or otherwise reproduced without his/her permission.

L'auteur a accordé une licence irrévocable et non exclusive permettant à la Bibliothèque nationale du Canada de reproduire, prêter, distribuer ou vendre des copies de sa thèse de quelque manière et sous quelque forme que ce soit pour mettre des exemplaires de cette thèse à la disposition des personnes intéressées.

L'auteur conserve la propriété du droit d'auteur qui protège sa thèse. Ni la thèse ni des extraits substantiels de celle-ci ne doivent être imprimés ou autrement reproduits sans son autorisation.

ISBN 0-315-63214-3

LASER DEBONDING OF CERAMIC ORTHODONTIC BRACKETS

BY

ROBERT MAURIZIO TOCCHIO

A thesis submitted to the Faculty of Graduate Studies of  
the University of Manitoba in partial fulfillment of the requirements  
of the degree of

MASTER OF SCIENCE

© 1990

Permission has been granted to the LIBRARY OF THE UNIVERSITY OF MANITOBA to lend or sell copies of this thesis, to the NATIONAL LIBRARY OF CANADA to microfilm this thesis and to lend or sell copies of the film, and UNIVERSITY MICROFILMS to publish an abstract of this thesis.

The author reserves other publication rights, and neither the thesis nor extensive extracts from it may be printed or otherwise reproduced without the author's written permission.

## TABLE OF CONTENTS

	<u>Page</u>
ABSTRACT.....	iii
ACKNOWLEDGMENT.....	iv
LIST OF FIGURES.....	v
LIST OF TABLES.....	vii
INTRODUCTION.....	1
REVIEW OF LITERATURE.....	3
Orthodontic Bonding.....	3
Ceramic Brackets.....	6
Lasers: Historic Review.....	16
Laser and Light Theory.....	20
Lasers and Dental Hard Tissues.....	24
Thermal Considerations.....	31
Statement of Purpose.....	37
MATERIALS AND METHODS.....	38
Spectrographic Analysis.....	38
Laser Debonding Experiments.....	40
Thermal Evaluation.....	48
RESULTS.....	51
Spectrographic Analysis Results.....	51
Laser Debonding Results.....	60
Damage Evaluation.....	66
Thermal Evaluation Results.....	71
DISCUSSIONS.....	74
Temperature Measurements.....	83
Enamel and Bracket Damage.....	86
Sources of Error.....	88
CONCLUSIONS.....	90
FUTURE RESEARCH.....	91
BIBLIOGRAPHY.....	95
APPENDIX 1 (Light and Laser Theory).....	105
APPENDIX 2 (Basics of Spectroscopy).....	122
APPENDIX 3 (Pilot Study Results).....	132
APPENDIX 4 (Raw Data).....	134

## ABSTRACT

The introduction of ceramic orthodontic brackets has further compounded the problems associated with debonding. The increased bonds strengths obtained with ceramic brackets has resulted in an increased incidence of enamel damage. Laser light transmitted to the bracket/adhesive interface can be used to degrade the bonding resin by either thermal or photochemical processes.

The efficacy of lasers in removing brackets safely, without enamel or bracket damage, without thermal damage to the pulp and in a clinically satisfactory time was determined. The influence of various laser wavelengths (193, 248, 308 and 1060 nm) and various bracket types (Starfire, Transcend) on debonding effectiveness was also examined. Debonding times, material damage, site of bond failure and pulpal temperature rise were correlated to absorption spectra of the adhesives and bracket types.

Sapphire brackets can be debonded more quickly than Polycrystalline (PC) brackets because they allow greater light energy to reach the adhesive. Ultraviolet wavelengths are more effective for bracket removal than 1060 nm irradiation with 248 nm being most effective. These results correlate well to the absorption spectra of the adhesive. No enamel or bracket damage was observed and little or no force is required to remove the brackets. For the laser parameters used in this study, the pulpal temperature increase is acceptable with the sapphire brackets but not with the PC brackets. Laser debonding appears to be a thermal process at low pulse energy levels and an ablative process with increased pulse energies.

## ACKNOWLEDGEMENT

To my research advisor, Dr. Peter Williams, Department of Rehabilitative Dental Sciences, for his knowledge, support and guidance, and the ability to temper the many ups and downs of this project.

To my external examiner, Dr. Ken Standing, Professor, Department of Physics, for his laser expertise, for advice throughout the bulk of this work and for allowing a 'dentist' to invade his lab.

To Dr. Franz Mayer, Department of Physics, for his valuable input during the early experimentation. "Cheers" to my German friend.

To Ed Kammermyer and staff, at the Ontario Lightwave and Laser Research Center, Toronto, Ontario, for numerous valuable suggestions and the outstanding facility at which the bulk of the experimentation was performed.

To Daryl, in Biostats, for guiding me through the 'Mac' and helping me deal with the graphics nightmare.

To Dr. Ed Yen, for advice and assistance along the way and for listening when the 'wall' seemed most insurmountable.

To Dr. Robert Baker, for his wealth of knowledge in clinical orthodontics. Thanks for trying to teach me what you know.

To the many people at Unitek-3M and A-Company, for their assistance and the donation of the many ceramic brackets needed for this project.

To my new, trusted and cherished friends, Arthur and Fred. The many good times we've shared are priceless and will never be forgotten. A lifetime of friendship is ours to share.

## LIST OF FIGURES

<u>Figure</u>	<u>Page</u>
1. Stress vs strain for sapphire and steel.....	9
2. a. Chemical structure of a silane b. Bonding of silanes to surfaces.....	11
3. Enamel 'tearout'.....	14
4. External transmission for sapphire.....	15
5. Properties of coherent light.....	20
6. IR spectra of lased and nonlased enamel.....	24
7. Absorption spectra of enamel.....	26
8. Bracket transmission set-up; laser.....	40
9. Mounting jig; side view.....	43
10. Mounting jig; top view.....	43
11. Completed sample with orientation mark.....	44
12. Sample mounted in holding apparatus.....	44
13. Laser debonding set-up; 248/308 nm.....	46
14. Laser debonding set-up; 1060 nm.....	47
15. Thermocouple set-up.....	49
16. UV\VIS spectra of Dynabond.....	51
17. IR spectra of Dynabond.....	52
18. UV\VIS\NearIR spectra of Dynabond (Hitachi)..	53
19. IR-UV spectra of Dynabond (Carey).....	54
20. PC bracket spectra.....	54
21. S bracket spectra.....	54
22. Sapphire window spectra.....	55
23. Quartz window spectra.....	56
24. Silane spectra (on quartz).....	56

List of Figures cont'd

<u>Figure</u>	<u>Page</u>
25. Elemental analysis; PC bracket body.....	58
26. Elemental analysis; S bracket body.....	58
27. Elemental analysis; PC bonding surface.....	58
28. Elemental analysis; S bonding surface.....	58
29. SEM: Sapphire bracket fracture surface.....	59
30. SEM: PC bracket fracture surface.....	59
31. Elemental analysis; PC 'amorphous layer'.....	60
32. SEM: S bracket debonding pattern (15x).....	68
33. SEM: S bracket debonding pattern (200x).....	68
34. SEM: S bracket debonding pattern (500x).....	69
35. SEM: PC bracket debonding pattern (15x).....	70
36. SEM: PC bracket debonding pattern (500x).....	70
37. Potential 'degradable' adhesive spectra.....	92
38. "Sandwich" technique for bracket removal.....	92



## LIST OF TABLES

<u>Table</u>		<u>Page</u>
1.	Laser transmission of brackets.....	57
2.	PC bracket removal times; 248 nm laser.....	61
3.	S bracket removal times; 248 nm laser.....	61
4.	S/PC bracket removal times; 193 nm laser.....	62
5.	PC bracket removal times; 308 nm laser.....	63
6.	S bracket removal times; 308 nm laser.....	63
7.	PC bracket removal times; 1060 nm laser.....	64
8.	S bracket removal times; 1060 nm laser.....	64
9.	Temperature measurements; PC brackets.....	71
10.	Temperature measurements; S brackets.....	72
11.	Modes of energy dissipation for molecules....	77

## INTRODUCTION

The debonding of orthodontic brackets requires the removal of both bracket and residual adhesive. It may be time consuming and frequently results in some degree of enamel damage. The amount of enamel damage is a function of the forces required to remove the brackets, the bond strengths between enamel-adhesive-bracket, and the use of hand instruments (dental chisels, hatchets) and rotary instruments and abrasive pastes to remove the remaining resin. Patient demand for improved esthetics during orthodontic therapy resulted in the premature introduction of 'ceramic' brackets prior to completion of adequate research. Unfortunately, subsequent clinical experience with 'ceramic' brackets has demonstrated that the brittleness of the bracket and increased bond strengths at the bracket-adhesive interface further compounds the debonding problems seen with metal brackets. Possible solutions for safer and more predictable bracket debonding include modifying the existing procedure through bracket-adhesive manipulations, including using unfilled bonding resins and mechanical versus chemical retention or developing alternative mechanisms such as electrothermal debonding. However these solutions may result in decreased bond strength and the possibility of thermal damage, so they may not provide a satisfactory solution to the problems inherent in currently practiced debonding techniques.

Brackets made of alumina ceramic materials have the unique ability to transmit radiant energy in a wide range of wavelengths. Therefore laser energy should be able to be used to debond 'ceramic' brackets since laser light energy can be deposited directly at the bracket-adhesive interface.

This study validates the concept of laser debonding of ceramic orthodontic brackets. Debonding times, in conjunction with an assessment of enamel and bracket damage, pulp chamber temperature rise and absorption spectroscopy of the materials involved was performed. A hypothesis regarding the mechanism of laser debonding is proposed. The results of this study suggest directions for future research.

## REVIEW OF LITERATURE

### Review of Orthodontic Bonding

The direct-bonding of orthodontic brackets to etched enamel has become widely employed by orthodontists since being introduced more than two decades ago.<sup>1,2,3,4</sup> The primary concern in the development of orthodontic adhesives has been the development of adequate bond strengths between the bracket, adhesive and etched enamel surfaces. Tensile<sup>5,6,7,,</sup> shear<sup>8,9,10,</sup> torquing and peel tests<sup>11,12</sup> have been devised to evaluate the bond strengths in vitro and mimic the force systems present during active orthodontic treatment. In addition to the inherent strength of the brackets, bonding agents and enamel, other factors have been identified as having a direct influence on the strength of orthodontic bonding. Some of these are; the bracket base surface area<sup>13</sup>, base design<sup>4,14</sup>, base mesh size<sup>11,13,14</sup>, thickness of resin layer<sup>15,16</sup>, filler content<sup>5,8</sup>, effect of sealing agents<sup>17,18</sup> water sorption<sup>19</sup>, thermal cycling<sup>20</sup> and technique related factors.<sup>21</sup>

In order to ensure successful orthodontic bonding, the forces applied during treatment must not exceed the bond strengths of the tooth-adhesive-bracket complex. The force that is exerted will be composed of forces generated by the activation of the appliance and those arising from mastication. The maximum force has been estimated to be between 30 kg\cm<sup>2</sup> to 70 kg\cm<sup>2</sup><sup>9,22</sup>. Others<sup>23</sup> have estimated that a minimum of 9 kg is

exerted on the bracket ( $\approx 54 \text{ kg/cm}^2$  based on  $4 \times 4 \text{ mm}$  bracket area) during orthodontic treatment. In the study by Yamada et al<sup>24</sup> comparing the bond strengths of various bonding adhesives, values were never below  $80 \text{ kg/cm}^2$  and ranged to a maximum of  $176 \text{ kg/cm}^2$ . Keizer et al<sup>9</sup> found the enamel-adhesive bond strength to be  $1.21 \text{ kg/mm}^2$  or  $121 \text{ kg/cm}^2$ . It appears from these results that such bond strengths are more than sufficient to withstand various intra-oral forces and have facilitated the trend towards decreasing bracket size in recent years. Increased bond strengths will likely result in a greater frequency of enamel damage as they approach or even exceed the reported average enamel tensile strength of  $100 \text{ kg/cm}^2$ <sup>25</sup>. Note too however, that the reported strength of enamel is only an average and does not take into account qualitative differences such as hypocalcified and altered enamel structure or the effect of crystal orientation in strength testing. Therefore, enamel damage could occur at much lower force levels.

A number of difficulties in bonding\debonding procedures have been identified. These include loss of enamel due to etching<sup>26,27</sup> prior to bracket placement, fracturing<sup>26,28,29</sup> during bracket removal, retention of resin tags which can yellow with age and discolour the tooth<sup>26,29</sup>, corrosion of metal brackets resulting in staining at the bracket interface<sup>30,31</sup>, a roughened enamel surface which can result in increased plaque retention subsequent to debonding procedures<sup>28,32,33</sup> and a softer enamel surface with lower fluoride content more disposed to

decalcification<sup>34</sup>. Many of these effects are accepted by the clinician<sup>35</sup> who feel that they are insignificant.

The most frequently observed bond failure occurs at the bracket-adhesive interface<sup>5,7,10,36</sup>. If the bond strengths are high, failure will more often occur intra-adhesive or at the enamel-adhesive interface<sup>37</sup> resulting in enamel damage or 'Tear Outs'. This type of failure is observed when the bracket-adhesive interface bond is enhanced either by etching<sup>38</sup> or coating the bracket base with porous metal powder<sup>14,39</sup>. Bond strengths were seen to improve from 66.9 kg/cm<sup>2</sup> for untreated bases to 169 kg/cm<sup>2</sup> for the treated bases. Since debonding occurs at the weakest link in the bracket-adhesive-tooth complex, spot weld defects on the base surfaces of metal brackets have been shown to encourage fracture at the bracket-adhesive interface in spite of high bond strengths<sup>13</sup>.

With the increasing esthetic demand for smaller brackets and therefore smaller bonding bases, the gap between those bond strengths which are high enough to stand up to clinical treatment and yet, are still weak enough to avoid iatrogenic tooth damage, has narrowed considerably. Ideally, if brackets could be debonded safely, easily and predictably, a clinician would desire the highest possible bond strength. This high bond strength would decrease the incidence of bonding failures and improve clinical efficiency. Perhaps Sheridan<sup>40,41</sup> had this in mind when he introduced an electrothermal debonding device. He may simply have wanted to prevent damage during debonding in those situations

where the bond strength equalled or exceeded the enamel strength. His cordless battery operated device generates heat which is transferred to the metal bracket by a blade placed in the bracket slot. The metal bracket conducts heat efficiently while the underlying adhesive is a relatively poor conductor of heat. Thus, the adhesive at the interface can be thermally softened and the bracket can be gently lifted off the tooth. The thermal ramifications of this technique to the pulp will be addressed in a subsequent section. In this context however, Sheridan must be credited for devising an alternative mechanism for metal bracket removal. The gap between bond or enamel strength and the force required for bracket removal has been substantially widened using Sheridan's technique. After debonding, residual adhesive is removed from the tooth by conventional hand and rotary instruments both of which have the potential to damage the enamel.

### Ceramic Brackets

The search for improved esthetics in orthodontic appliances has always been active. As early as 1964 Newman's<sup>42</sup> introduction of polycarbonate brackets provided improved esthetics. The bond strengths reported<sup>43</sup> were superior to those of the metallic brackets available at that time. Unfortunately, since the polymeric brackets were prone to clinical fracture and creep<sup>44</sup> their clinical performance was unsatisfactory<sup>45</sup>. Subsequent development of metal reinforced plastic brackets<sup>46</sup> failed to

overcome these deficiencies.

The 'ceramic' bracket has recently been introduced to orthodontics. Ceramics are a broad class of materials which, although they contain both metallic and non-metallic elements, are neither metallic nor polymeric. They are renowned for their hardness and resistance to high temperatures and chemical degradation<sup>47</sup>. Their major disadvantage is their lack of ductility which renders them brittle and subject to sudden and catastrophic failure. Currently all dental ceramic brackets are composed of either polycrystalline or monocrystalline aluminum oxide. The former is made by sintering aluminum oxide powder at temperatures near 1800 °C. The monocrystalline aluminum oxide<sup>47</sup> is commonly called a sapphire and is formed by melting aluminum oxide ( $T_f < 2100^\circ\text{C}$ ) and then slowly cooling it to grow a single crystal. Both the polycrystalline and single crystal 'blanks' are milled into their final form by either diamond cutting or by ultrasonic cutting techniques.<sup>47</sup> Sapphire brackets are transparent while polycrystalline brackets have a translucent, ivory white to opaque appearance.

The optical properties and strength of polycrystalline ceramics are incompatible. Since transparency increases with grain size and since strength decreases once the grain size increases over 30  $\mu\text{m}$  current ceramic brackets are formed by fusing aluminum oxide particles of 0.3  $\mu\text{m}$ . to produce brackets with grain size of 20-30  $\mu\text{m}$ .<sup>47</sup>

The tensile strength of sapphire is significantly greater



than that of annealed or cast stainless steel alloy (1800-2600 MPa psi vs. 350 MPa)<sup>48</sup>. In contrast Polycrystalline brackets actually may be slightly weaker than metals in tension<sup>47</sup>. The tensile strength for metal is a bulk related phenomenon and because of the metal's ductility, it is virtually independent of small surface defects. In contrast, the brittle material alumina is highly dependent on surface defects. Sapphire brackets possessing high tensile strengths, have very low transverse strengths and cannot withstand impact loading<sup>47</sup>. Surface defects such as cracks act as centers of stress concentration. In brittle materials, the crack remains sharp since there is no plastic deformation occurring to enable blunting. As such, stress concentration of several orders of magnitude can develop at the tip of the crack. Once the stress exceeds a critical level the crack will begin to self propagate and result in spontaneous failure.<sup>49</sup>

The measure of a material's ability to resist fracture is known as fracture toughness. Figure 1<sup>48</sup> is a plot of stress versus strain for sapphire and stainless steel. While the tensile strength of sapphire is much greater than steel, the % elongation (elastic and plastic deformation to failure) is 1% and 20% respectively. Since energy is defined as force times distance the area under a stress\strain curve gives an indication of the material's toughness before fracture. It is apparent, from Fig 1, that significantly less energy is required to fracture sapphire than for stainless steel.

Figure 1.48

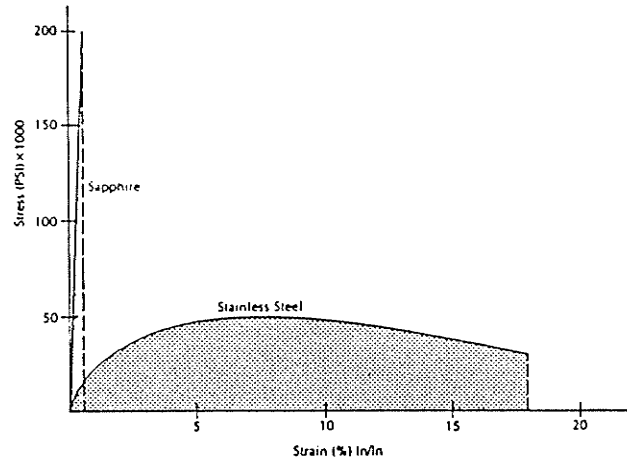


Fig. 1 Stress-Strain curves for sapphire and stainless steel. The height of the curve shows force loading, or strength. The horizontal axis shows strain, or distortion, under that load. Dashed vertical lines indicate failure (fracture) under load. The area under the curve is a rough indication of fracture toughness, or the total energy loading required to cause failure.

The units used to measure fracture toughness are the stress in Mega-Pascals (mega-Newtons/M<sup>2</sup>) and the strain in meters. The length of the surface crack enters into the formula as the square root meter<sup>48</sup>. Values of fracture toughness<sup>48</sup> for stainless steel, polycrystalline alumina and sapphire are; 80-95 MPa/M, 3.0-5.3 MPa/M, and 2.4-4.5 MPa/M. Note that even though the tensile strength of polycrystalline alumina is much less than sapphire it is a tougher material and can resist fractures better than sapphire.

For the clinician, low fracture toughness of ceramic brackets can drastically reduce the load required for fracture. Although the hardness of ceramics is 2-3 times greater<sup>47</sup> than stainless steel, surface defects introduced during manufacture orduring regular appointments can dramatically reduce their strength. A clinician must inform the patient of possible 'spontaneous' bracket fracture and the possibility of ingesting sharp ceramic particles.

The hardness of ceramics can be detrimental if grinding is required to remove a fractured bracket from a tooth. Although diamond is the hardest substance known to man, and diamond cutting instruments are commonly used in dentistry, cutting alumina with a diamond instrument will still be clinically time consuming. Therefore every effort should be made to prevent fracture of ceramic brackets by minimizing the deleterious forces exerted during treatment and during debonding procedures.

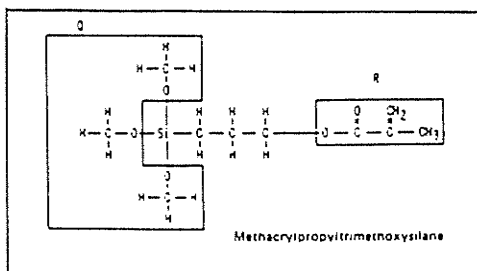
Another problem has been identified by investigators<sup>50,51,52</sup> who have reported rapid and dramatic abrasion of enamel caused by ceramic orthodontic brackets. Although thoughtful and judicious bracket placement by the orthodontist should decrease such occurrences, the clinician should remember that using brackets of such hardness and in the case of the polycrystalline brackets, surface roughness, results in enamel wear. Kusy<sup>53</sup> has suggested glazing or chemically treating the bracket surface to decrease roughness and reduce the coefficient of friction.

Alumina oxide cannot be directly bonded to the acrylic materials used for orthodontic bonding. Until recently bonding of ceramic brackets was achieved through the presence of undercuts of various designs on the bracket bonding surface. Bond strengths of these brackets are comparable or less than those of metal brackets<sup>54,55</sup>. Buzzita et al.<sup>55</sup> argued that filled adhesives were less able to flow into the retentive areas of the bracket base thus explaining the higher bond strengths obtained with unfilled resin adhesives. Odgaard and Segner<sup>56</sup> postulated that

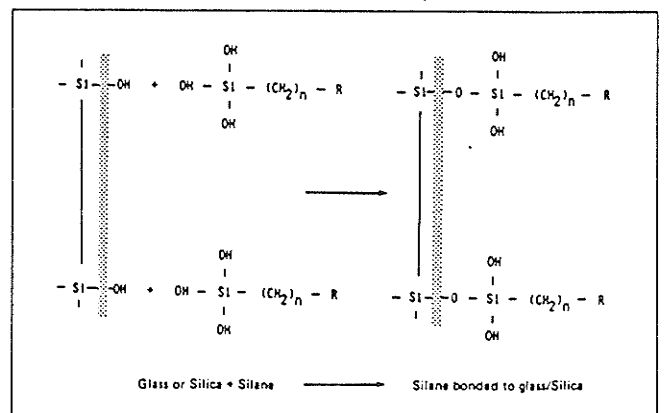
during curing of adhesives, the resin will contract and give rise to internal stress around the sharp corners of the grooved base. As a result the ultimate bond strength will be reduced. Iwamoto et al.<sup>57</sup> demonstrated that bond strengths would decrease as mechanical retention (# of grooves) was increased. The bond failure site of these brackets remains predominantly at the bracket-adhesive interface and within the adhesive<sup>56</sup>.

More recently chemical bonding of adhesive to the bracket base has been achieved by treating the aluminum oxide base with a silane coupling agent. This technology was pioneered by Bowen<sup>58</sup> who foresaw the advantages of using filler particles which would couple to the resin matrix to produce a reinforced (composite) polymer network. The most common coupling agent in use is a methacrylate terminated silane,  $\gamma$ -methacryloxypropyl-trimethoxysilane<sup>59</sup>, Figure 2a. This coupling agent bonds to the ceramic via the hydroxyl (usually silanol-SI-OH) groups to form a monolayer of silane with the methacrylate groups projecting from the surface, Figure 2b. These will then co-polymerize with the resin during setting.<sup>59,60</sup>

Figure 2 a,b.<sup>60</sup>



Chemical structure of commonly used silanes: Q = hydrolyzable group of silicone, e.g. alkoxy or acetoxy group R: organofunctional group selected for compaubility with the resins.



Bonding mechanism of silane to glass or silica surfaces.

The same chemical bonding mechanism has been successfully employed for bonding acrylic to porcelain. Bond strengths are reported<sup>61,62,63</sup> to be comparable or to exceed those for metal brackets, especially when the porcelain surface is roughened by grinding before treating with the silane primer. As bond strengths increased, so too did the incidence of porcelain fracture during debonding.<sup>61,62,63</sup>

While it appears that increased roughening (mechanical retention) can result in increased bond strength to porcelain, the same may not be true of silanized ceramic brackets having mechanical retention. Studies by Iwamoto et al.<sup>57</sup> and Slomka and Powers<sup>37</sup> found increased bond strengths with these silanized brackets while Newman et al.<sup>64</sup> and Buzzitta<sup>55</sup> questioned the clinical effectiveness of silane application to increase the bond strength of mechanically retained ceramic brackets. Guess et al.<sup>65</sup> found that even though the silanization of mechanically retained ceramic brackets had no significant effect on bond strengths, fracture occurred almost exclusively at the enamel-resin interface rather than at the bracket-adhesive interface. The retention of a bracket with this design it appears, was strong enough to override any possible effects of base silanization.

A number of manufacturers have recently switched to ceramic brackets which rely exclusively on chemical bonding of the acrylic resin. Only a few published reports comparing their shear bond strengths to those of metal brackets are available.

Gwinnett<sup>66</sup> and Odegaard and Segner<sup>56</sup> have both found superior bond strengths with the chemically bonded brackets and have noted that bond failure occurs predominantly at the enamel-resin interface. High bond strengths are attributed to the chemical bonding, a lack of internal stress in the resin and lack of bracket flexure during debonding as occurs with the metal brackets<sup>56,66</sup>. Joseph and Rossouw<sup>67</sup> in a most recent report found the debonding shear force of ceramic bracket groups to be significantly higher than those of stainless steel brackets regardless of whether light or chemically cured resins were used. An average force of 28.3 MN/M<sup>2</sup> was required for the highest ceramic bracket group while 17.8 MN/M<sup>2</sup> was enough to debond the strongest metal bracket group. The site of failure for the ceramic brackets was dominantly at the enamel-adhesive interface. Enamel fractures occurred in 40% of the chemically cured resin and ceramic bracket group. Another 7% of ceramic brackets fractured during removal.

With the advent of chemically bonded ceramic brackets it seems apparent that bracket-adhesive failures are no longer found. Rather, the limiting factor in the enamel-adhesive-bracket complex has shifted to the enamel-adhesive interface. The ramifications of such a shift are vividly illustrated in the published report by Newesely and Rossiwall<sup>52</sup>. Utilizing X-ray SEM elemental analysis they show a high frequency of enamel tearouts in a wide range of sizes. The largest tearout found measured up to 1.5 mm in diameter, Figure 3.

Figure 3.<sup>52</sup>

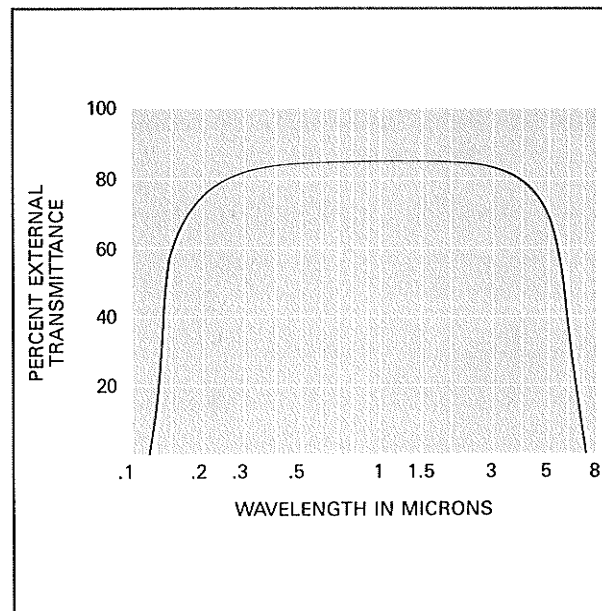
The ceramic bracket industry enthusiastically entered into the practice of orthodontics in response to the strong demand created by the bracket's optimal esthetic appeal. Unfortunately, the problems of bracket fracture, enamel abrasion and possible enamel tearouts encountered after their introduction has led many practitioners to question the efficacy of using this product. Unitek has recently converted all their chemically bonded ceramic brackets to mechanically bonded brackets by sintering silica particles to the bases. They did however, possess the technology to alter the bonding strength of the chemical ceramic bracket through direct manipulation of the number of active silane bonds<sup>23</sup>. Another ceramic bracket manufacturer is pursuing the possibility of utilizing the electrothermal debonding device (pers comm.) in an effort to improve the acceptability of the ceramic bracket into orthodontic practice.

Increased bond strengths should result in improved bracket retention rates and the production of smaller more esthetic brackets. Decreasing the force needed for debonding can decrease bracket fracture and eliminate lengthy clean up and provide a

controlled and less destructive bonding location. ETD (electrothermal debonding) may represent a mechanism by which the gap between bond strength and debonding force can be widened. Pulpal damage however, may be a limiting factor. The lower thermal conductivity of alumina oxide will likely result in longer debonding times and excess heating of the tooth and pulp prior to debonding.

It is apparent from the foregoing that debonding of ceramic brackets continues to be a problem for the clinician, manufacturers and patients. Ceramic brackets are formed of alumina oxide which has been shown to transmit a wide range of radiant energy, Figure 4. This special optical property may facilitate debonding through the use of lasers.

Figure 4.<sup>68</sup>



EXTERNAL TRANSMITTANCE FOR SAPPHIRE of 1mm thickness.



### Lasers - Historic Review

It has been said that the laser is a solution looking for a problem, rather than a development in response to a specific need<sup>69</sup>. The growth in the number of laser applications has been almost exponential. Einstein discovered the theoretical background for the laser in 1917<sup>70</sup> but it was not until 1960 when Theodore Maiman of Hughes Aircraft, now credited as the inventor of the laser, applied the theory to create the ruby laser.<sup>70</sup>

Surprisingly lasers have been involved in dental research since 1963<sup>71</sup>. Many specific areas of laser applications in dentistry have been identified. Some of these are; surgical treatment of oral malignancies and lesions, treatment of periodontal disease, caries prevention, detection and control, endodontics, prosthodontics, biostimulation, tooth desensitization, analgesia, in-vivo welding, storage of radiographic and 3-dimensional images, etc. As existing systems are refined and new laser systems are introduced a plethora of potential applications will be conceived. As yet, there have been no reports of lasers applied specifically to the field of orthodontics.

From only three citations in the 1964 edition of the Index to Dental Literature, dental laser reports have grown to over 70 in the 1988 Index. Less than one-fifth of these citations are in English. In 1986 there were only four dental professionals listed as members of either the International or American Societies for Laser Medicine and Surgery. The emerging importance of dental

laser research warranted a World Congress on Lasers in Dentistry during 1988, in Tokyo, Japan.

Historically, Leon Goldman in 1965<sup>72</sup> is credited with the first in vivo report of laser application to a healthy, living human tooth. The patient reported no pain when a maxillary second molar was exposed to two direct impacts by a ruby laser (694 nm). The tooth was extracted and sent for microscopic study. Only superficial destruction of the crown occurred. Another study by Stern and Sognnaes<sup>73,74</sup> showed how that laser irradiation of enamel appeared to decrease enamel permeability to acidic fluids. Some<sup>75</sup> claimed that the ruby laser was not suitable for cavity preparation because of potential pulpal damage due to the energy levels needed to remove dental hard tissues. Further advances would have to await the introduction of newer laser instruments.

Lobene et al.<sup>76</sup> in 1968 were the first to use the CO<sub>2</sub> laser for dental application. Their attempts to fuse pits and fissures as a means of caries prevention demonstrated how the mid-infrared wavelength (10.6  $\mu$ m) of the CO<sub>2</sub> laser produced different thermal effects than did the ruby laser. CO<sub>2</sub> irradiation also caused small amounts of hydroxyapatite to be converted to the more insoluble calcium orthophosphate apatite. Kantola<sup>77</sup> has provided a detailed description of macroscopic, microscopic and X-ray diffraction studies of CO<sub>2</sub> irradiated enamel and dentin while Melcer<sup>78</sup> has demonstrated caries removal with dentin healing and reparative-dentin formation.

Laser research on dental tissues in the United States has suffered greatly during the mid to late 1970's as a result of several published reports<sup>75,76</sup> which minimized the potential of future research. Grant funds evaporated and potential researchers turned their efforts to other fields while the laser was gaining substantial research acceptance in many medical, bioengineering, communication and industrial applications. As a result, American laser research in dentistry has fallen well behind that in other countries. Rather than being in the forefront of dental laser application, dentistry receives most of its new laser technology second hand from the medical profession.

A large amount of literature has accumulated since the first report of the surgical (soft tissue) application of a CO<sub>2</sub> laser<sup>79</sup>. Surgeons claim many advantages of surgery using a laser; a bloodless field, shorter and less traumatic procedures and less post-operative pain and edema. Unlike the CO<sub>2</sub> laser, the light from the recently introduced Nd:YAG (Neodymium:Yttrium-Aluminum-Garnet) laser operating in the near infrared, 1.06  $\mu$ m, can easily be transmitted fibreoptically into a small handpiece. Applications include 'Laser Scalpels' which can perform precise bloodless cutting, removal of caries in enamel and fusing of enamel for caries prevention<sup>80</sup>. Recently this type of laser has been specifically manufactured and marketed to the dental profession by the American Dental Laser Corp<sup>81</sup>. Whether this laser possesses enough suitable characteristics to remain in the

dental laser field will depend on further research and a favorable comparison to alternative laser systems. Researchers in Japan<sup>82</sup> have developed a hollow, metal lined, flexible tube to transmit CO<sub>2</sub> radiation into a handpiece. This new development may be enough to allow the CO<sub>2</sub> laser to supercede the clinical use of the Nd:YAG laser.

A new class of lasers, the excimer laser, operating in the ultra-violet (UV) range (100-400um) was introduced to the dental field in 1987<sup>71</sup> following its application in the fields of ophthalmology, cardiac surgery and orthopaedics. Excimers allow extremely sharp and precise tissue cutting without thermal damage because of their ability to ablate material by photo-decomposition. These new lasers may prove valuable to the dental profession.

## Laser Theory and Light Interactions with Matter

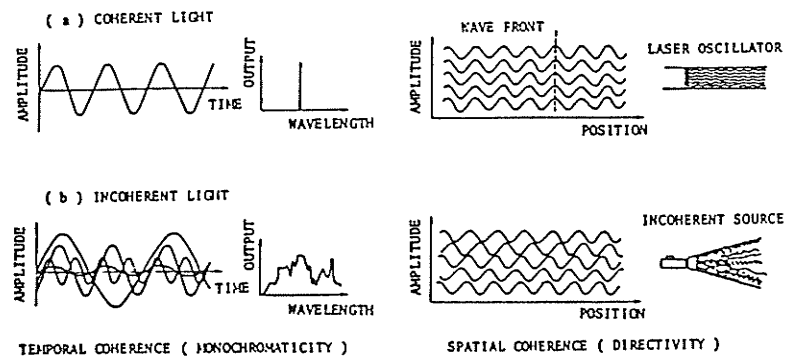
A basic knowledge of laser characteristics as well as the mechanism by which light interacts with matter are mandatory if an individual wants to interpret the results of many laser experiments.

The word LASER is an acronym for 'Light Amplification by Stimulated Emission of Radiation'. The basic differences between lasers and other light sources are the characteristics of the light emitted from a laser. They are;

1. Synchronicity (phase coherency)
2. Monochromaticity (frequency coherency)
3. Directivity (spatial coherency)
4. Excellent concentration of energy (high photon density)
5. Extremely high brightness.
6. Controllability.

The coherent properties in time and space are compared to incoherent light in Figure 5.

Figure 5.<sup>83</sup>



Temporal and spatial property of coherent light from a laser compared with those of incoherent light from a conventional light source

In contrast to incoherent light, light waves emitted from a laser have the same amplitude and are in phase. Conventional light sources emit light over much of the visible and infrared spectrum while for all practical purposes, the laser can be considered monochromatic, containing a beam of very narrow range wavelengths. The divergence of a laser beam is very small, about a milliradian (approximately  $0.05^\circ$  divergence). As a result of being focussed and synchronous, the output power can be concentrated to produce a small high intensity and a high energy density beam. In addition, by pulsing the laser, the energy can be released over a shorter time to give very high power pulses rather than relatively low but constant power emitted by a continuous wave (CW) laser. A more detailed discussion of the nature of light and the mechanism of laser action are found in Appendix 1.

When electromagnetic energy (light) comes into contact with matter it can either be reflected, transmitted or absorbed and then scattered or refracted within the material. The study of the interaction of light with matter is known as spectroscopy. A great deal of information can be gleaned by knowing the wavelengths of photons that an organic molecule can absorb most efficiently. The energy ( $E$ ) associated with a photon is related to the frequency ( $f$ ) of the light by the following formula  $E=hf$ , where  $h$ =Plancks constant ( $6.6 \times 10^{-34}$  joules/sec). As the frequency increases so does the photon energy. Accordingly a photon of Ultraviolet (UV) light will have much more energy than a photon

of Infrared (IR) light. The energy absorbed by a molecule or atom can be resolved into at least four major components; translational energy, rotational energy, vibrational energy and electronic energy. The translational energy level is essentially continuous and represents the lowest energy of the molecule or atom. For each of remaining components there are certain discrete, permissible energy levels. An atom does not absorb any photons unless the photons have enough energy to bring about the transition from one energy level to another. Only those photons which carry the exact amount of energy required for transition to the next permitted level, can be absorbed. Electronic transitions require much more energy than vibrational transitions which in turn require much greater energy than rotational transitions.<sup>84</sup>

$$E_e \gg E_v \gg E_r$$

Consequently, rotational transitions are accomplished by considerably less energetic photons, and by Planck's equation, longer wavelength radiation such as microwaves. Vibrational transitions require photons in the infrared region, and electronic transitions need the more powerful photons associated with short wavelength radiation such as visible and ultraviolet radiation. In contrast, the passage of IR radiation through a material can increase the various energy levels of the atom or molecule efficiently only when radiation of the correct frequency to cause a vibrational or rotational change is absorbed. Spectroscopic study of organic compounds is therefore, in essence, an investigation of the types of waves that can be

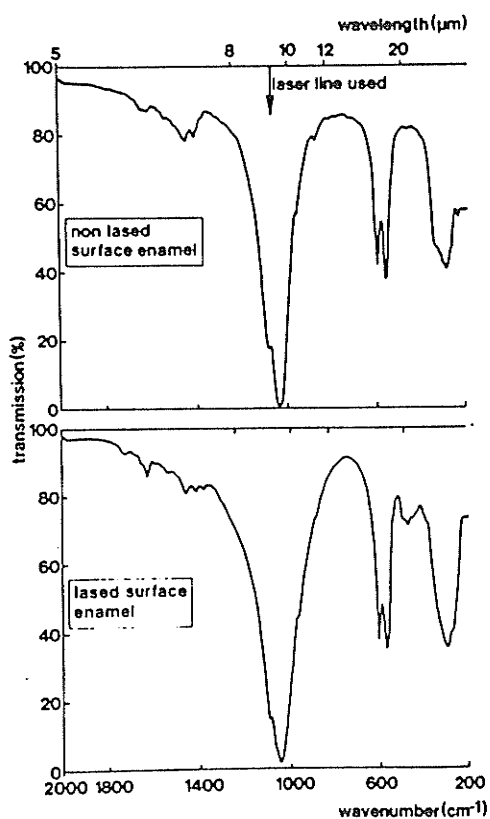
absorbed efficiently by a compound. Spectra may thus give an indication of what lasers may best be suited for a specific purpose. (NB. further explanation of spectroscopy and light\matter interactions, with emphasis on UV and IR regions are found in Appendix 2). Spectroscopic information should indicate which laser wavelengths would be highly absorbed, allowing the desired result with as low a laser power as possible. Since low power will result in both a lower cost and lower incidence of undesired thermal effects, identification of these 'resonant' wavelengths is very desirable to maximize the laser effect.



## Lasers and Dental Hard Tissues

The effect of CO<sub>2</sub> laser irradiation on enamel and dentin tissues is well documented. The radiation is highly absorbed on the surface of enamel or dentin with low depth of penetration. Many IR spectroscopic studies have been performed on enamel and hydroxyapatite crystals<sup>85,86</sup>.

Figure 6.85



IR spectra of lased and nonlased surface human enamel in KBr pellets in the region (200-2,000  $\text{cm}^{-1}$ ). The enamel was lased with the 1,073  $\text{cm}^{-1}$  line and a pulse energy density of 50  $\text{J} \cdot \text{cm}^{-2}$ .

The spectra obtained show a very strong absorption band in the vicinity of 10.6  $\mu\text{m}$ ., the same wavelength at which the CO<sub>2</sub> laser operates. Many CO<sub>2</sub> lasers are 'tunable' and can operate at several closely related wavelengths. Laser irradiation in this region of the mid-IR spectrum is strongly absorbed by the phosphate ions in the hydroxyapatite of the tooth enamel<sup>87</sup>. The resulting vibrational excitation results in great heat generation and surface vaporization even with low laser energy levels.

Strong surface absorption will minimize laser penetration and maximize the rate of surface heating. The latter will allow the surface to vaporize before enough time has elapsed for heat

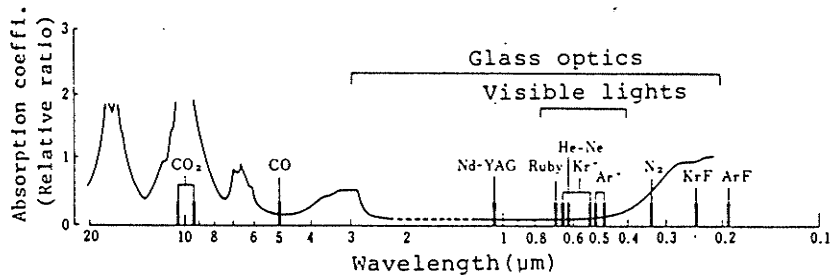
diffusion into the tooth. Both of these will reduce adverse pulpal response. Moreover Fowler and Kurada<sup>87</sup> speculate that the use of selected wavelengths which coincide with specific ion absorption wavelengths of enamel will result in desired chemical reactions. For example, the selective excitation of the OH group to higher energy levels may promote Fluoride ion diffusion along the apatite channels<sup>87</sup>. In an artificial caries study Stern et al.<sup>88</sup> found that the higher absorption of enamel for 10.6 um. irradiance compared to 0.694 um (ruby laser) irradiance allowed them to use 1/15th the energy density to produce similar levels of protection of enamel against demineralization. Clearly, knowledge obtained through spectroscopic investigation of how light reacts with a material is critical to selection of the most appropriate laser for a specific purpose.

Perhaps the most dramatic example of appropriate laser selection, based on a material's properties and desired results, is that used by ophthalmic surgeons in the repair of detached retinas. Based on a lack of interaction with corneal material and a selective absorption by the retina, an Argon laser (488 green or 514.5 blue) can be used to 'spot weld' a detached retina back to its base without damaging the cornea or lens of the eye. Such a finding was not likely based on spectroscopic analyses of cornea, lens and retina but more likely on common sense. The fact that humans see colors, the visible part of the electromagnetic spectrum, indicates a significant proportion of light (in the visible range) must be transmitted through the

cornea and lens to the retina. The selective absorption of one tissue versus the selective transparency of another tissue has revolutionalized ophthalmic surgery.

While mid-infrared spectroscopic data on enamel is abundant, the literature is virtually devoid of information regarding the interaction of UV, Visible or near IR electromagnetic radiation with enamel. The effectiveness of various laser systems are often measured by comparing the energy densities needed to obtain a specific result. Morioka et al.<sup>89</sup> include one of the few spectra of enamel absorption in the UV to IR regions. They demonstrate that tooth enamel is virtually transparent to wavelengths between the visible and near IR spectrum. Light from Nd:YAG, ruby, and krypton lasers are essentially not absorbed by enamel. Light from carbon dioxide, carbon monoxide in the IR and krypton-fluoride, argon-fluoride and nitrogen lasers in the UV are however, remarkably more absorbed.

Figure 7.<sup>89</sup>



Wavelength of lasers and the absorption spectra of human tooth enamel

While it would appear that CO<sub>2</sub> laser radiation is much more suitable for use on enamel, the Nd:YAG by American Dental Laser Corp. has become the first laser specifically marketed to the dental profession because of the relative ease with which the radiation can be fibre optically transmitted. Realizing the relatively weak absorption of Nd:YAG laser light by enamel and dentin, the manufacturers are advocating its use in conjunction with a black ink painted on the hard tissue. Results of future studies coupled with the continued emergence and refinement of laser technology may, in the future conclude that the Nd:YAG laser system was prematurely mass marketed. Boehm<sup>90</sup> states that up to 40% of incident radiation at wavelengths 1.25um or lower is reflected by the enamel surface.

Figure 7 demonstrates that enamel absorbs well in the UV range of the electromagnetic spectrum. When ultraviolet light interacts with matter, it affects the electronic state of atoms and thus has the ability to promote chemical reactions including dissociations, see Appendix 2. IR lasers melt and vaporize material via thermal processes. The very high melting point of human enamel (1280°C)<sup>91</sup> makes it nearly impossible to remove or cut enamel without significantly increasing the potential for thermal pulp damage. UV excimer lasers however, are able to photodecompose<sup>92,93</sup> organic and inorganic material with only limited thermal effects<sup>93</sup>. A highly energetic photon will induce bond cleavage producing molecular fragments and elemental compounds. Energy not consumed in bond breaking is converted into

kinetic energy by expansion of the resulting gaseous phase and the decomposition products are blown off with ultrasonic speed. Frentzen et al.<sup>94</sup> using a 193 ArF excimer laser demonstrated conclusively, through mass spectroscopy techniques, that enamel and dentin can be ablated. Photoablation in their study is a tissue specific process with the demineralized zones of a carious defect being ablated much more rapidly than unaffected areas. The lowest ablation rate was found in the mineralized zone on the floor of carious lesions in dentin.

Several papers demonstrating the ablative effects of 248nm KrF<sup>95</sup> and 308 XeCl<sup>96</sup> excimer laser radiation on bone have been published recently. Yow's study<sup>96</sup> showed a thermal damage zone of only 2-3 um in bone tissue surrounding the ablated zone. This width represents only a tenth of a diameter of a single cell and is much less than either the thermal ablation zones of 5-11 um created by the 2.9 um Erbium:YAG laser<sup>97</sup> or the 600 um zone created by the CO2 laser<sup>97</sup>. The authors also demonstrated the ablation of a bone cement composed of polymethylmethacrylate and styrene. Again the thermal damage zone of 10-40 um caused by 308 nm excimer is significantly less than the zone of 375 um caused by the Erbium:YAG<sup>97</sup>.

Only two reports can be found describing the dental application of the 308 nm excimer laser. Pini et al.'s<sup>98</sup> use of the 308 excimer laser in root canal therapy demonstrated that demineralized (infected) dentin was preferentially ablated compared to sound dentin. The sound dentin acts as mechanical

guidance as the optic fibre was inserted into the canal ablating infected dentin. The rate at which the fibre proceeded was constant and slowed dramatically where much of the dentin was healthy. A smaller diameter fibre was then inserted to continue down the canal. Microscopic examination revealed a smooth clean canal of constant size corresponding to the fibre size.

Hame et al.<sup>99</sup> have recently studied the effect on enamel of the 308 excimer laser operating at 20 Hz and employing a 600  $\mu\text{m}$  fibre size. The authors measured the diameter and depth of holes created when varying the energy densities (50,70,90,  $\text{mj}/\text{mm}^2$ ) and exposure (500,1000,1500,3000,4000 pulses). The depth of penetration initially increased linearly with increasing number of pulses and the ablation rate increased with increasing energy density. The most rapid rate of penetration into enamel appears to occur during the first 500 pulses. Regardless of energy density, the penetration rate then drops significantly from 0.30  $\mu\text{m}/\text{pulse}$  to 0.05  $\mu\text{m}/\text{pulse}$ . The authors do not specifically offer an explanation for this finding but infer it could be related to the slight divergence of laser beam seen at higher depths. No differences were found between human and bovine enamel during lasing.

Interesting results have been found with the Erbium:YAG which is another recently released laser system. Unlike the excimer lasers which operate in the UV end of the spectrum, the Er:YAG is an infrared laser operating in the mid-IR region at 2.94  $\mu\text{m}$ . Unique to this laser is its strong absorption by tissue

water. A study<sup>100</sup>, comparing the skin ablative effects of a 308 nm XeCl excimer laser and a pulsed Er:YAG laser demonstrated the Er:YAG to be very effective in tissue removal by ablation. Less thermal damage was seen with the Er:YAG relative to the 308 excimer laser. Direct comparisons between the two systems were difficult because the lasers operate at very different parameters. The XeCl excimer, with 20 nanosecond (ns) pulse width was tested between 5-50 Hz while the Er:YAG has emission duration of 250 us. Each 250 microsecond (us) pulse is composed of single energy spikes occurring at 1 us intervals. Repetition rates of only 5 Hz can be obtained with the Er:YAG. Due to strong absorption of tissue water at 2.94 um radiation the Er:YAG laser appears able to rapidly ablate tissue without thermal consequences.

As yet only two groups<sup>101,102,103</sup> have investigated the effects of Er:YAG irradiation of dental hard tissues. Unlike the CO<sub>2</sub> laser which tends to melt and vaporize hydroxyapatite crystals, the Er:YAG laser is absorbed strongly by interstitial water. As the water within the surface layer of the tooth vaporizes, high pressure is generated resulting in microexplosive removal of enamel or dentin. Temperature increase is much less (16.1°C)<sup>103</sup> than with CO<sub>2</sub> lasing (>1300°C)<sup>104</sup> and is more localized. Hibst and Keller<sup>101</sup> demonstrate that while the depth of cratering is in linear proportion to the number of pulses of irradiation for dentin, the depth in enamel is not directly related to pulse number. Reduced cutting rate in enamel could be

due to dentin's higher water content (enamel  $\approx 2.5\%$ , dentin  $\approx 13.5\%$ ). The ablation effect of the Er:YAG has been described as threshold dependant ie; irradiation above a certain energy density will result in ablation while energy densities below this will result in heating effects. Paghdiwala<sup>103</sup> believes the use of a Q-switched (see Appendix) Er:YAG will increase ablation efficiency and result in even lower temperature increases.

#### Thermal Considerations

The acceptance of lasers into the dental profession will be based on their effectiveness and efficacy. Those lasers which can achieve similar or improved results compared to current dental procedures and prove cost and time effective will be viewed as desirable. The use of dental lasers must be shown to be biologically safe to the patient and the clinician. Lasers which can meet these criteria will likely be widely adopted by the profession.

When considering the use of dental lasers for debonding brackets, the potential thermal damage to vital pulps must be evaluated. Several investigators<sup>105,106,107</sup> have attempted to correlate intrapulpal temperatures, to histologic results. Lisanti and Zander<sup>105</sup> placed a thermocouple in a prepared buccal cavity of a vital tooth in a dog. The heat source was applied for 5 or 60 sec. giving an enamel surface temperature range from 51.6-315°C. A temperature rise at the pulpal-dentino junction (PDJ) of 1.9-24.7°C for the 5 second exposure test and 7.5-50.8°C



for the 60 second test was recorded. The thickness of dentin ranged between 0.81 mm to 1.82 mm and all cavities were subsequently filled with zinc eugenol cement. Surprisingly enough the authors report that not one pulp death was found. While elevations in pulp temperature correlated well with the severity of pulpal injury, healing occurred in every case. The stages of the recovery process are; walling off of an area of injury, then removal of necrotic tissue, followed by the replacement of damaged tissue and finally the deposition of irregular dentin opposite the irradiated tubules. Research by J.F. Cox<sup>108</sup> has shown that if the pulp is sealed off from the oral environment, full pulp recovery, including deposition of reparative dentin occurs even after a major insult which results in necrosis of the pulp adjacent to the site of injury.

The results reported by Zach and Cohen<sup>106</sup> on a similar set of experiments on the teeth of Rhesus Macaca monkeys differ dramatically from Lisanti and Zanders. The tip of a soldering gun kept at constant temperature, 275°C was applied to the enamel surface of a tooth for periods of 5-20 seconds, long enough to obtain pulp temperature increases of 2-17°C. Histologic examination showed that 15% of pulps exposed to a temperature rise of 5.6°C showed necrosis and at 11°C over 60% of teeth were necrotic. All pulps heated by 17°C became necrotic. The disparity between the above studies are certainly dramatic and elude explanation. Although there were differences; species, enamel vs.dentin, temperature measurement methods, zinc oxide filling

etc, some procedural error must exist in either study to explain such large discrepancies.

Nyborg and Brannstrom<sup>107</sup> have examined the reaction of the human pulp to heat. Cavity preparations were drilled into 29 sets of contralateral premolar teeth scheduled for orthodontic extraction. A temperature of 150°C was applied for 30 seconds. Dentinal thickness ranged from 0.02 mm to 1.10 mm. All cavities were restored only with amalgam. At one month histologic results showed all test teeth had sustained some pulpal injury resulting in the deposition of low differentiated predentin. Only four teeth displayed cellular changes suggesting necrosis. All teeth were asymptomatic. No measurement of intrapulpal temperatures were obtained. Such findings seem more closely related to those of Lisanti and Zander. The authors suggest that the rich blood supply of these young pulps might well have diminished greater thermal injury.

The discussion above serves to illustrate the imprecision with which thermal insult has been correlated to pulpal response. Notwithstanding the foregoing imprecision, one can say with some degree of confidence, that pulpal temperature increases of up to 5.6°C (10°F) should be well tolerated and not result in irreversible damage to the pulp. Further increase however, may result in damage with subsequent repair and regeneration or result in pulpal necrosis. Ideally any pulpal effect should be avoided. In a article reviewing thermal trauma to teeth<sup>109</sup> it appears that pulpal temperature increase in excess of 10°F was

not found for any of the commonly performed dental procedures.

The pulpal effects of various lasers have also been investigated. Adrian et al.<sup>75</sup> attempted to establish energy density thresholds for pulpal response using the ruby laser. Dog teeth that were irradiated with a single laser shot were extracted 48 hours after exposure. Many teeth displayed necrosis with no surface effects. The ruby laser, they concluded, was not suitable for preparation of cavities. The authors did not however, investigate the possibility of repair and regeneration by examining teeth after a healing period. These authors went on to demonstrate a lower incidence of pulpal necrosis when teeth were exposed to similar energy densities of Nd:YAG radiation<sup>110</sup>.

The precise mechanism by which lasers exert their effects on pulpal tissue is still very much unresolved. Shoji and Woriuchi<sup>111</sup> using argon, CO<sub>2</sub> and Nd:YAG laser irradiation of whole rat teeth, demonstrated calcified tissue formation and increased alkaline phosphatase activity. Melcer et al.<sup>112</sup> have found similar stimulation of dentin formation after CO<sub>2</sub> laser exposure of deep Class V lesions. Dentinogenesis occurred between 800 and 8000 J/cm<sup>2</sup>, above which they found necrosis which was unresolved three months later. Direct pulpal exposure to CO<sub>2</sub> radiation can also result in reparative dentin formation<sup>113,114</sup>. The origin of the odontoblastic activity observed is not clear but could result from either repair and regeneration by cellular differentiation after thermal insult or from direct laser activation of the cell. The strong surface absorption of CO<sub>2</sub>

radiation leads one to suspect that thermal effects stimulate odontoblastic activity.

Launay et al.<sup>115</sup> have recently attempted to quantify the thermal effects of Nd:YAG, argon and CO<sub>2</sub> laser on enamel, dentin and dental pulps by means of computerized infrared thermography and thermocouples. Thermal results showed a very low absorption of the Nd:YAG beam by enamel and dentin. Energy at this wavelength was transmitted to the pulp. Overheating of the pulp is in a direct ratio to the applied power. External and internal temperature rise and lack of surface alteration demonstrate how 1060 nm irradiation diffuses through hard tissues to the pulp. The small external temperature rise is consistent with absorption of a small amount of incident energy. The authors do not advocate the use of a continuous wave Nd:YAG on hard tissues without the use of a surface absorbent. The results obtained for argon laser irradiance were inconsistent and depend on whether the enamel surface is clean. An argon beam is strongly reflected back by clean enamel. According to Boehm<sup>90</sup> wavelengths lower than 1.25  $\mu\text{m}$  are reflected more than 40% by dental enamel.

Very high surface temperatures and very low pulpal temperature increases were found with CO<sub>2</sub> irradiation of dentin or enamel. External temperatures of approximately 1230°C<sup>115</sup> are sufficient to melt hydroxyapatite. These temperatures are in the same order as those reported elsewhere<sup>104</sup>. Pulpal temperature increases were below the thresholds of 5.6°C established by Zach and Cohen.<sup>106</sup> Others<sup>116</sup> have reported similar pulpal temperatures

with single shot CO<sub>2</sub> irradiation. A thermal threshold exists below which no overheating is noticed in the pulp chamber. Beyond this threshold, pulpal overheating grows directly with laser energy deposition<sup>115</sup>.

It would appear from the above that the CO<sub>2</sub> laser could be used dentally without pulpal damage. Bearing in mind however, that all of the above studies were performed with a single shot exposure. Total tooth heating during a dental procedure using a laser will likely be related to a number of factors including; total time of irradiation, repetition rate, pulse duration versus refractory time, spot size, energy density, use of coolants, wavelength of irradiation-absorption coefficient, pulpal blood flow, heat sink effects of alveolar bone and PDL etc.. Temperature measurements should be made for each dental procedure performed with the various lasers utilized in order to establish the effect on a per procedure basis.

### Statement of Purpose

The main objectives of this study are to investigate the potential for debonding ceramic orthodontic brackets using various wavelength lasers;

1. Determine the efficacy of lasers in removing brackets safely, without enamel or bracket damage, without thermal damage to the pulp and in a clinically satisfactory time.
2. Examine the influence of various laser wavelengths and various bracket types on debonding effectiveness.
3. Attempt to correlate debonding times, material damage, site of bond failure and pulpal temperatures to absorption spectra.
4. Propose a mechanism for the observed results.

## MATERIALS AND METHODS

### I SPECTROSCOPIC ANALYSIS

#### A. IR and UV Absorption Spectra of Adhesives

Since the effectiveness of laser interaction with the bonding resins will be strongly dependent on the absorption of the laser radiation by the resin, an absorption spectroscopic analysis was performed. Several commercial adhesives (Challenge, System I, Monolok, Achieve and Dynabond) used for bonding orthodontic brackets, were prepared according to the manufacturer's directions. The freshly prepared adhesives were placed between two siliconized glass slides and compressed to form thin films, ranging in thickness from about 50 to 350  $\mu\text{m}$ . When set, the films were separated from the slides and subjected to spectroscopic analysis with a Hewlett-Packard 8452 UV\Vis Diode Array Spectrophotometer<sup>®</sup> with microprocessor and a Perkin-Elmer IR Spectrophotometer.<sup>®</sup>

Dynabond, the adhesive utilized for the laser debonding portion of the study was further analyzed using a Hitachi U2000 Double beam Spectrophotometer\* which analyzed absorption between 190-1100 nm and the Carey 14<sup>+</sup> spectrophotometer which analyzed absorption between 2.5  $\mu\text{m}$  and 300 nm. These spectra were obtained with a silane agent (Ormco Porcelain Primer) added to the adhesive. The silane was added in order to evaluate the possibility of a synergistic absorption effect of both reactive components. A UV through visible light spectra (190-820 nm) was also obtained for Bis-GMA polymer.

---

<sup>®</sup> Department of Chemistry, Univ. of Manitoba

\* Department of Biochemistry, Univ. of Manitoba

+ Department of Engineering, Univ. of Manitoba

## B. IR and UV Transmission Spectra of Brackets

1) As a reference standard, the spectrum from a standard grade sapphire window (2.0 cm diameter X 2.5 mm deep) was obtained (General Ruby and Sapphire Corp.), using the Hewlett-Packard Spectrophotometer.

2) To determine any differences that exist between the transmission spectra for sapphire (S) and polycrystalline alumina (PC) brackets, transmission spectra were determined, and compared to each other and to those spectra published for sapphire. Spectra were obtained using the Hewlett-Packard 8452 UV\Vis Diode Array Spectrophotometer (190-820 nm). Masking devices constructed of thick black cardboard were made to conform to each bracket type (S-A Comp, PC-Unitek) to assure that all light reaching the photodetector had passed through the bracket. Prior to obtaining bracket spectra, a reference spectrum was obtained with the masks and no bracket in place.

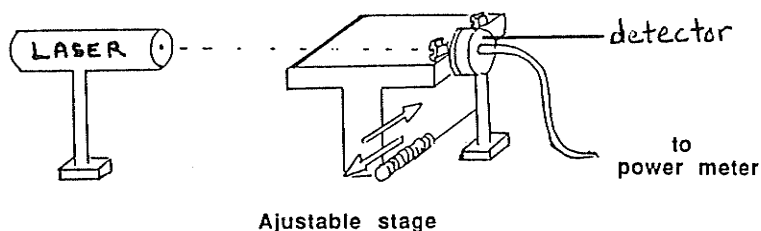
3) In order to determine how much light passes through the bracket to the adhesive layer, the light transmission characteristics of the brackets were determined. One sapphire and one polycrystalline bracket were placed on the edge of a moveable stage, Figure 8. The bracket surface faced the laser. The base, hanging over the edge of the stage, faced the optical power meter detector (Newport Corporation). The detector was placed as close as possible to the bracket in an effort to read all light passing through the base and to minimize loss due to scatter. A continuous wave Helium-Neon laser at 632 nm and a continuous



wave argon laser at 488 and 514.5 nm were used. The apparatus was aligned so that a light beam 1 to 1.5 mm in diameter struck the center of the bracket surface at 90°. Power readings of the incident beam and of the transmitted beam were taken. All tests were performed in darkness to eliminate the interference of ambient light. An attenuator was placed on the power meter when using the argon laser. These tests were performed at the Ontario Lightwave and Laser Research Center, in Toronto, Ontario.

Figure 8

#### BRACKET TRANSMISSION USING LASERS



4) Bracket composition and bonding surface characteristics were examined utilizing a JXA 840 Scanning Microanalyzer. Several of each bracket type were fractured and mounted for SEM element X-Ray analysis (EDAX). All elements with higher atomic weight than Oxygen could be detected.

## II Laser Debonding Experiments

### A Sample Preparation

Methodology for this group of experiments had been developed as a result of a pilot study. (Appendix 3). Primary Bovine teeth were extracted and stored in room temperature water.

Before bonding, the teeth were polished with pumice powder, washed, dried, and the enamel bonding surface acid etched according to the manufacturer's directions (60 sec with 30% Phosphoric acid, thorough water wash and dried). The use of Bovine enamel as a substitute for human enamel has been justified<sup>117,118,119</sup>. For each wavelength to be tested (193, 248, 308, 1060 nm), 15 brackets each of Unitek (PC) and A-Comp (S) were bonded to the bovine teeth with Dynabond (Unitek) according to manufacturer's directions and stored in water until testing. In spite of the fact that a previous pilot (Appendix 3) had shown that wet versus dry storage had no significant effects on laser debonding times, all samples were kept wet in an effort to more closely mimic clinical conditions. Since the results obtained in this pilot study showed that Unitek's Dynabond gave similar results to the other adhesives tested (System 1, Achieve, Challenge) and since Unitek brackets were involved in the study, Dynabond was used for the remaining experimentation.

The bonded tooth and bracket assemblies were mounted in Coe Quick Set tray acrylic. To ensure accurate and reproducible positioning of the bracket during debonding, a mounting jig was fabricated from clear acrylic (Fig. 9). The jig had a circular recess into which would fit tightly an 18 mm diameter brass metal ring. The ring was filled with Coe Quick set tray acrylic and seated into the recess. The bracket-tooth assembly was positioned in the jig so that the bracket remained free of the tray resin and was held in place by two 0.016 SS wires running through the

bracket (Fig. 10). After the tray acrylic had partially set, an orientation mark was placed into the tray acrylic to facilitate accurate positioning into a sample holder (Fig. 11). The mounting jig was removed prior to final set of the tray acrylic. Upon complete polymerization the acrylic samples were separated from the rings, trimmed and stored in room temperature water until testing. A wooden frame was constructed to serve as a sample holder during debonding. For testing, the sample is oriented in the frame and secured into place with a set screw (Fig.12).

## B Debonding Procedure

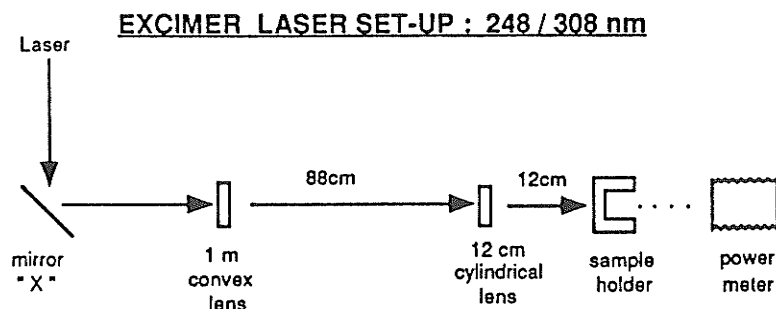
This portion of the experiment was performed at the Ontario Lightwave and Laser Research Center, in Toronto, Ontario. The main objectives were to examine the debonding effectiveness of various wavelengths of laser light. Fifteen PC and 15 sapphire (S) brackets were tested at wavelengths of 193, 248, 308 and 1060 nm. Samples were irradiated and the time until failure measured. A light constant shear force of  $8 \text{ kg/cm}^2$  was applied to the brackets during debonding. This force represents only a fraction,  $<1/10\text{th}$ , of debonding values reported in the literature<sup>24,56,66,67</sup>. The application of a light shear force was at this time deemed to be necessary from a clinical standpoint since the viscosity of a thermally softened resin might prevent debonding. In an effort to apply a similar shear stress to both the PC and sapphire brackets, compensations for the different bracket base areas were made. Both brackets were placed on an overhead projector and magnified. Acetate tracings were made of each magnified base and the weights were compared. The PC base was 0.7176x the size of the sapphire (S) base. Based on the formula for shear stress (shear load per cross sectional area parallel to the stress) the weight applied to the PC brackets was 730.5 gms while 1018 gms was applied to the sapphire (S) brackets to give an identical shear stress.

### 1. Laser parameters

In order to compare the debonding effectiveness of various wavelength lasers, an identical energy density (Energy/unit area)

must be delivered at each wavelength. Since the lasers used in these experiments differed from those used in the pilot experiments, a new set of laser parameters had to be determined. Only the polycrystalline brackets were used for this determination since the sapphire brackets gave unusual results. For the PC bracket determination, a debonding time of approximately 2-4 seconds/bracket was selected as we believe such times to be within clinically acceptable limits. To achieve this debonding time for PC brackets, the energy output (Watts or Joules/s) of the Lumonics Excimer 460-SMA laser operating with KrF gas at 248 nm was focussed to give a bonding surface spot size of 3.5x3.5 mm, and was set to 49 Hz for an average power level of 4 watts. The average power density at the bonding surface was calculated as approximately 32.6 watts/cm<sup>2</sup>. This energy density was maintained as closely as possible throughout the remainder of the experiment at each wavelength tested.

The apparatus set up for irradiation at 248 and 308 nm is shown in Figure 13.



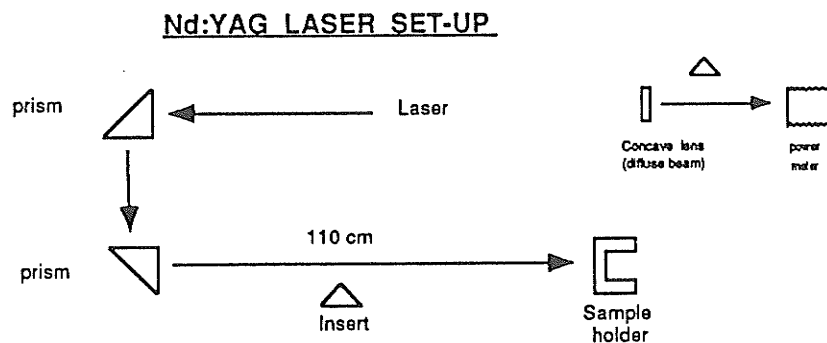
Vertical changes in the beam position were performed at the mirror ("X" in Figure 13). A one meter convex lens and a 12 cm

cylindrical lens were positioned to focus the beam to the desired spot size. Fifteen PC and 15 sapphire brackets were irradiated at 248 nm.

Several problems arose when using the ArF 193 nm laser. Since a cylindrical convex lens was not available to focus the beam horizontally at 193 nm, a 3.5 X 3.5 mm carbon mask was placed in front of the sample in an attempt to block out the unwanted portion of the beam. As this laser did not have a gas processor, ArF depletion occurred so rapidly that the laser could be operated for only thirty minutes per gas fill. At 118 Hz and 39.9 KV the maximum power obtained at the bracket after 60 sec of operation was only 1 Watt. Therefore only five of each PC and sapphire brackets were tested.

A Quantaray DCR-3 Q-switched Nd:YAG laser was used for irradiation at 1060 nm. Four watts of power was obtained and the laser was operated in the following configuration.

Figure 14.



The energy distribution within the beam was irregular. A 'hot spot' of approximately 2.5-3 mm diameter was centrally located and focussed on the bracket.

A digital stopwatch was used to measure all times. A response test was carried out for timing error determination.

### C Damage Evaluation

All debonded samples were collected, catalogued and inspected with a Zeiss binocular microscope at magnifications up to 40x for evidence of enamel damage and for determination of the site of fracture. A representative number of samples in each group were inspected using a JOEL-35C scanning electron microscope.

## III Thermal Evaluation

### A Sample preparation

In order for laser debonding to be considered efficacious the technique must not cause excessive temperature rise in the pulp. The methodology to measure pulp chamber temperature rise during laser irradiation was developed in a separate pilot project using bovine and human lower incisor teeth. Since human lower incisor teeth contain the smallest pulps of all human teeth and thinnest labial walls, laser debonding proven safe with those teeth will likely be safe with all other teeth.

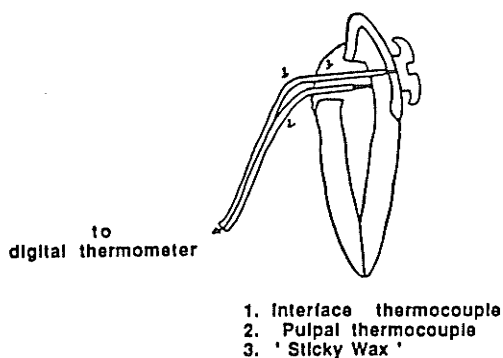
For each laser wavelength and bracket type, two teeth were prepared, one Bovine with bracket and one Human with bracket. The lingual surface of the tooth was cut away until the pulpal cavity was exposed. The cavity was thoroughly cleaned and a 700 FG dental bur was used to cut a hole for the thermocouple from

the pulpal wall through the labial dentin to the enamel layer. A 1/4 round bur was then used to extend the hole until it perforated the labial enamel. The thickness of the labial wall adjacent to the hole was measured with a pair of calipers. The labial wall thickness of bovine and human incisor teeth were very similar averaging about 2.0 mm (range was 1.5 to 2.3 mm). All mesial and distal surfaces were ground parallel so the teeth could be fixed in a vice like modification of the sample holder. All teeth were etched and stored in room temperature water until final preparation.

On the day prior to testing the prepared teeth were dried and the thermocouples were installed into the teeth. A Copper/Constantan Type PT (Sensortek Inc, New Jersey) thermocouple was inserted through the lingual access to the enamel surface. A bracket (PC or S) was then bonded onto the surface as previously described and the tip of the thermocouple was pushed into contact with the bracket-adhesive interface. A second thermocouple was placed in contact with the pulpal wall. Both were secured in place with molten 'sticky wax'. All prepared samples were stored in 100% humidity overnight.

Figure 15.

CROSS SECTIONAL VIEW  
OF THERMOCOUPLE SET - UP





## B Experimentation

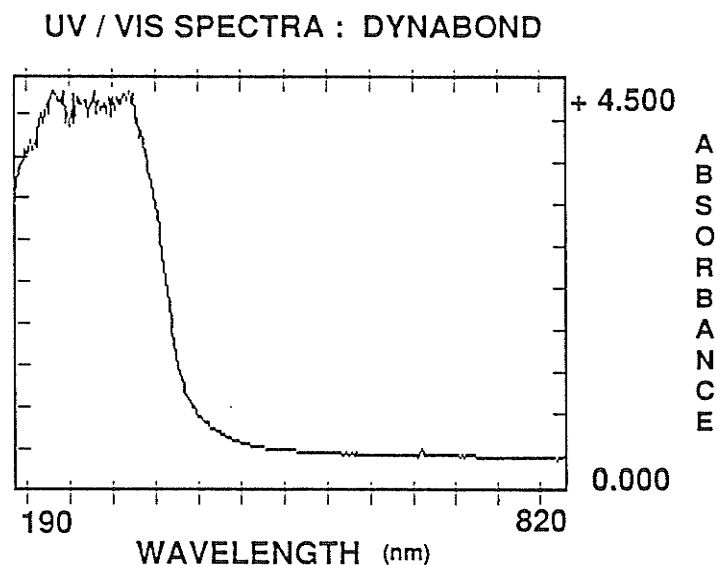
A tooth was inserted into the apparatus and aligned using very low 248 nm KrF laser power. The thermocouples were connected to the electronic digital thermometer (Bailey Model BAT 8, New Jersey). All temperature readings were converted to degrees Celsius. The initial (equilibrium) temperature was noted and the stop watch started as soon as the tooth was exposed to the laser light, using the identical parameters for power density and spot size used in the debonding study. Exposure continued for the average time of debonding as determined earlier. A reading from the bracket-adhesive interface was taken immediately after laser shut down and the measuring device was switched to read the pulpal thermocouple. Results of the pilot study demonstrated a time delay for reaching maximum temperature in the pulp as the thermal front slowly diffused through the tooth. Thus, the time at which the maximum pulp temperature is reached will occur after the digital thermometer is switched to the pulpal thermometer. Both the time to pulpal temperature maximum and the maximum temperature obtained in the pulp were recorded. Each tooth was tested five times after it had returned to the equilibrium temperature. The pilot study showed that the results of repeated tests were fairly consistent.

## RESULTS

Spectra of Adhesives

The spectra obtained for the various adhesives analyzed with the Hewlett-Packard 8452 UV\Vis Spectrophotometer all appeared very similar. A typical UV\Vis spectra (Dynabond) is shown in Fig 16. The remaining spectra are found in Appendix 4.

Figure 16.

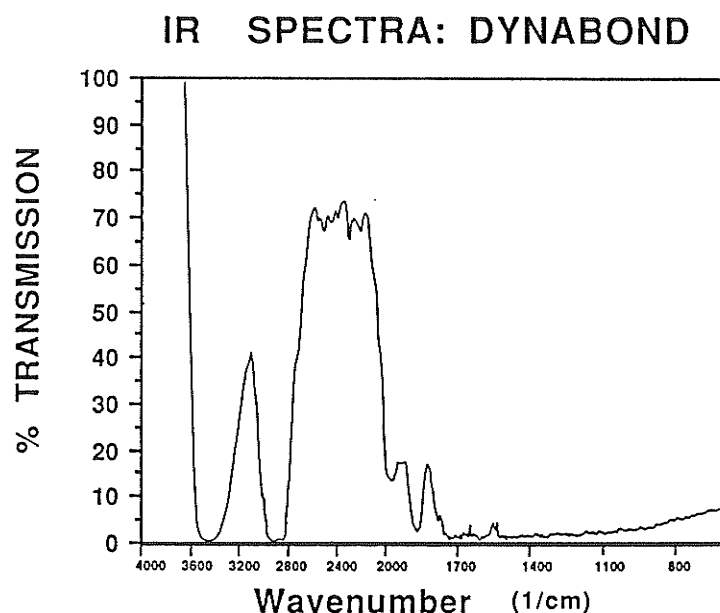


The vertical axis shows relative absorption and the horizontal axis shows the wavelength expressed in nanometers. All the adhesives strongly absorb light in the UV region of the spectrum at approximately 190-350 nm. Absorption rapidly decreases into the visible spectrum. The base line values of absorption are affected by the thickness of the film tested. Film thickness was not standardized. The adhesives had variable viscosities which, because of the method of fabrication, resulted in a variable thickness. The thinnest films, Bis-GMA and Dynabond, were clear

while other films appeared opaque. Qualitatively all the film spectra are very similar with strong UV light absorption and low visible light absorption.

A typical IR spectra of an adhesive (Dynabond) is shown in Figure 17. Again all the spectra obtained for the various adhesives tested are very similar. The remaining spectra are found in Appendix 4.

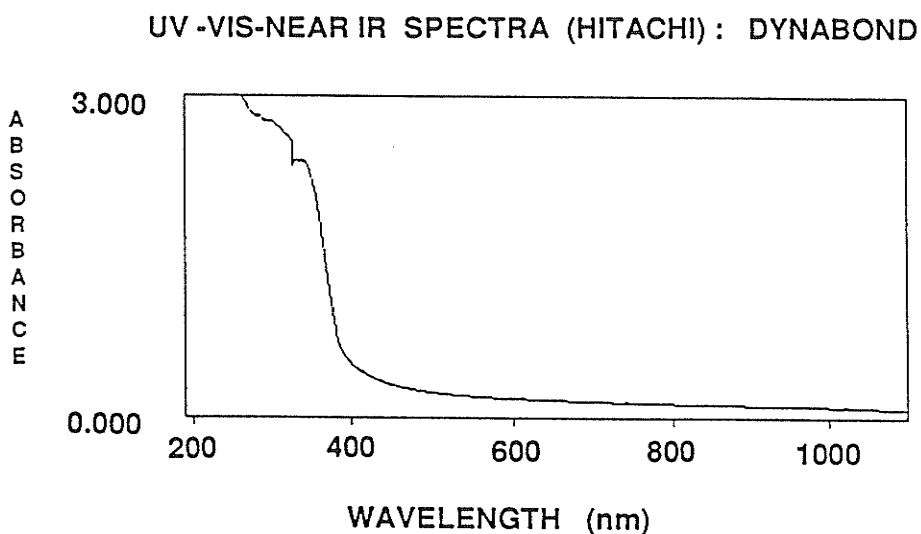
Figure 17.



The vertical axis is expressed as the % Transmission, while the horizontal axis is expressed as the Wavenumber ( $\text{cm}^{-1}$ ); the inverse of the wavelength expressed in centimeters. Strong absorption peaks occur in all samples between  $3600\text{--}3400\text{ cm}^{-1}$  ( $2.7\text{--}2.9\text{ }\mu\text{m}$ ) and  $2840\text{--}3000\text{ cm}^{-1}$  ( $3.3\text{--}3.5\text{ }\mu\text{m}$ ). The polymers differ slightly in the amount of transmission below  $3000\text{ cm}^{-1}$ , while a generalized lack of transmission occurs below  $1700\text{ cm}^{-1}$  ( $5.9\text{ }\mu\text{m}$ ).

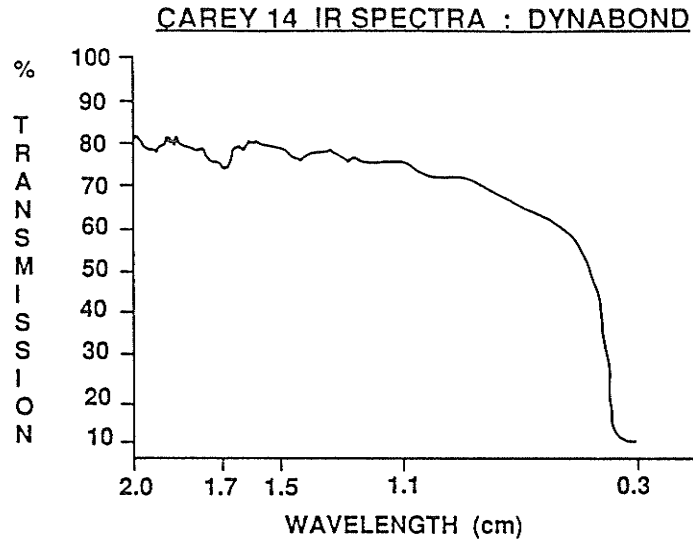
Spectral analysis of Dynabond (Fig 18) with silane (Ormco Porcelain Primer) on the Hitachi U2000 Double Beam Spectrophotometer gave very high absorption in the UV range and low absorption throughout the visible and near infrared spectrum to 1100 nm.

Figure 18.



Relative to the reference beam some light energy was absorbed at 1060 nm. Whether this energy was absorbed and/or reflected by the film could not be determined. Results obtained using the Carey 14 double beam spectrophotometer, Figure 19, shows the transmission spectra obtained between 300 nm and 2.0 um. Again, a high absorption occurs in the UV. A 20% proportion of the beam is not transmitted relative to the reference beam. This energy is either absorbed and/or reflected.

Figure 19.



Bracket Analysis

The spectra obtained for Unitek's polycrystalline bracket, A-Company's sapphire bracket and a standard grade sapphire window (Gen. Ruby and Sapphire Co.) on the Hewlett-Packard 8452 Uv\Vis Diode Array Spectrophotometer are shown below (Fig 20,21,22). Spectra of the accompanying masking device or reference are found in Appendix 4.

Figure 20

UV/VIS SPECTRA : PC BRACKET

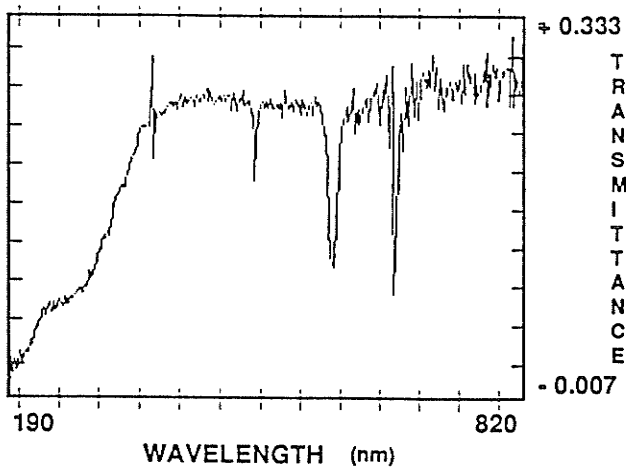


Figure 21

UV/VIS SPECTRA : SAPPHIRE BRACKET

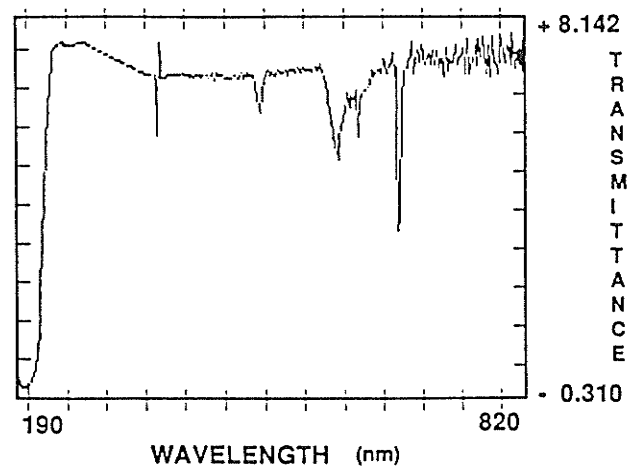
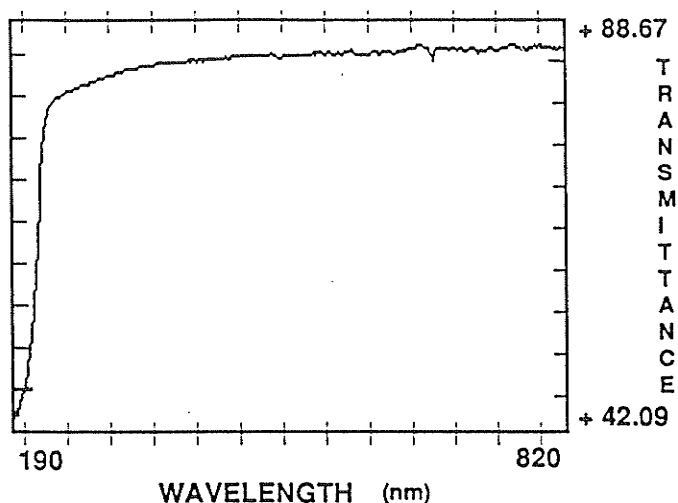


Figure 22 UV / VIS SPECTRA : SAPPHIRE WINDOW



Approximately 100% transmission occurred with the masks (Append.4). In comparing the sample spectra, the most obvious difference is seen in the % transmittance. While the standard sapphire window gives a transmittance of nearly 88.7 %, which is similar to those reported in the literature<sup>68</sup>, the maximum transmission for the sapphire (S) and polycrystalline (PC) brackets are approximately 8 % and 0.3 % respectively.

The shape of the sapphire bracket spectra is relatively similar to that of the sapphire window, showing a very strong drop in transmission starting at about 230 nm. The PC bracket displays a much more gradual drop in transmission starting at about 350 nm, with a shoulder at 225 and the lowest transmission around 200 nm. Both the PC and S bracket spectra show a number of accessory peaks not found on the spectra of the standard grade sapphire window. These peaks appear to be similar for both the PC and sapphire brackets and occur at 364, 486, 580 and 656 nm.

A scan of a quartz blank window, Fig 23, and of a common silanizing agent on the quartz blank, Fig. 24, have also been included in this section. Quartz is virtually transparent to all light between 190 and 820 nm while the silane agent appears to have slight absorption only at 225 nm and below.

Figure 23.

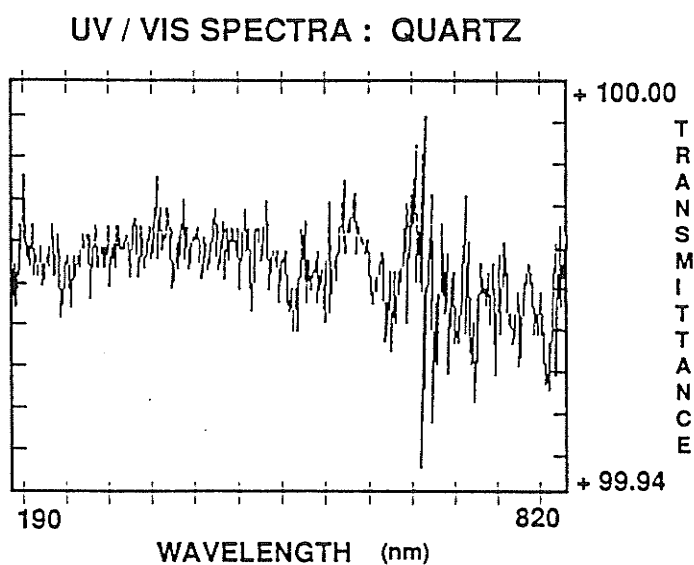
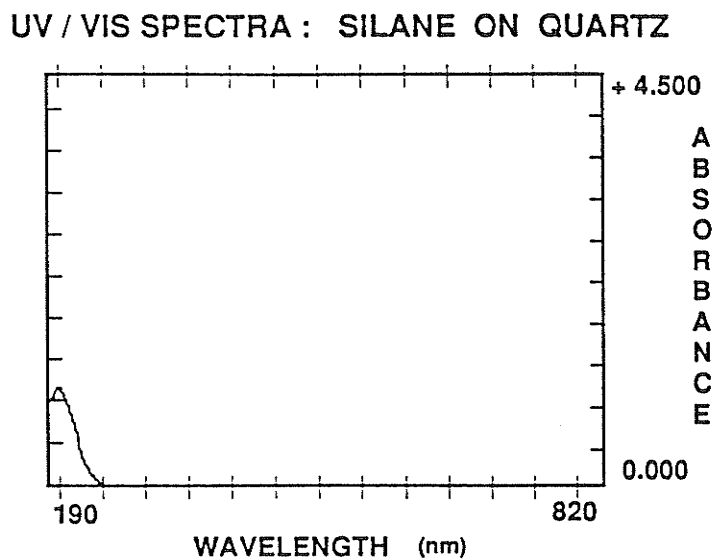


Figure 24.



The quantification of bracket transmission utilizing lasers was carried out in an effort to support or refute the % transmissions obtained in the preceding spectral analysis and in an effort to determine what level of transmission occurs with coherent light. Transmission values obtained and calculated percentages are listed for each laser tested in Table 1.

Table 1

	Helium/Neon 632 nm	Argon 488 nm	Argon 524 nm
Incident beam	1.70 mW	22.2 mW	30.8 mW
A-Comp (S)	1.45 mW (85.3%)	15.2 mW (68.5%)	20.2 mW (65.6%)
Unitek (PC)	0.46 mW (27.1%)	2.0 mW (9.0%)	3.3 mW (10.7%)

Note that with the Helium\Neon laser, the % transmission of S approaches that obtained for the sapphire window but is less with the Argon wavelengths tested. A possible explanation for the differences might include the observed laser power drift that was found for the Argon laser. Every attempt was made to record transmission during power peaks. As well the Argon beam was 0.5 mm larger than the 1.0 mm diameter Helium\Neon beam and as such was more likely to be affected by bracket surface geometry

Results of SEM X-ray analysis of the PC and S brackets are shown in Figs. 25,26. Only elements with greater atomic weights than oxygen and present in concentrations greater than 0.1 % will



be detected by the energy dispersive X-Ray analyzer. Within the limits of the instrument detection the bulk of both brackets are composed of pure Alumina. A silicon containing compound is present on the bonding surface of both brackets, Figures 27 and 28.

Figure 25

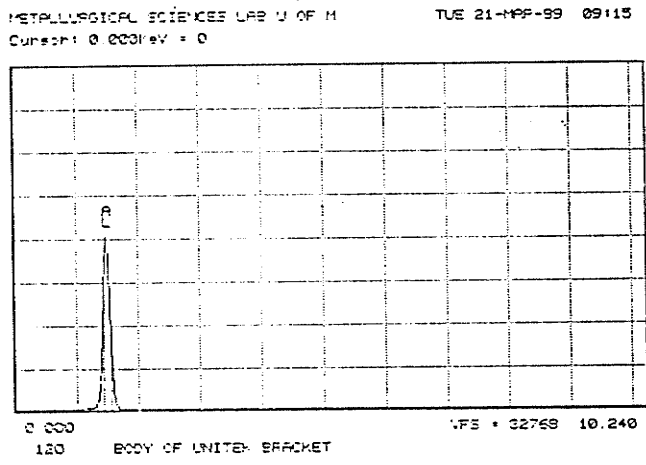


Figure 26

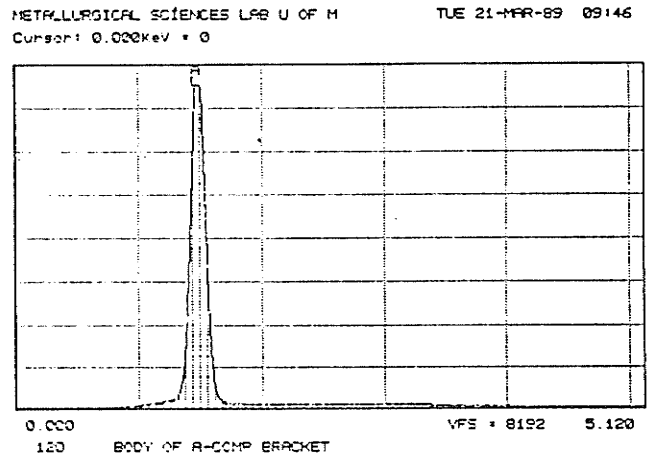


Figure 27

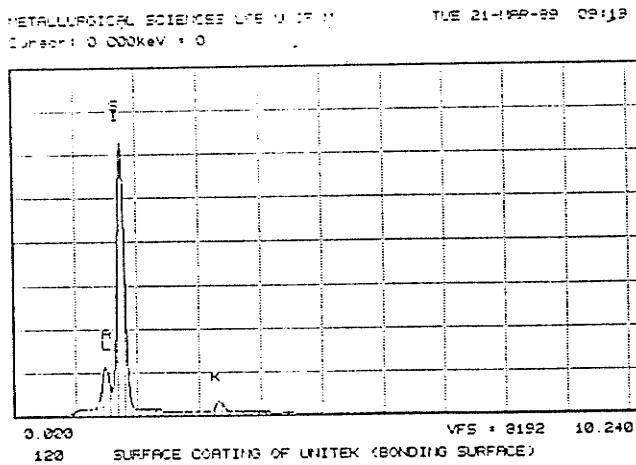
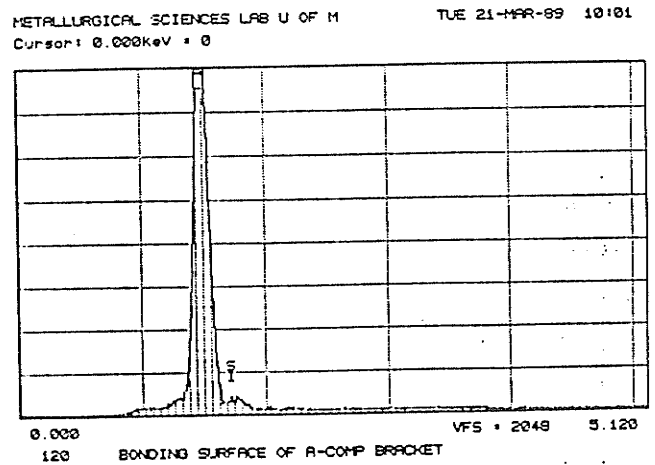


Figure 28



Photographs of the fracture surfaces, Figures 29 and 30, illustrate the polycrystalline nature of the Unitek bracket and the featureless, smooth surface of the monocrystalline A-Company

bracket. Individual crystal facets are clearly visible on the fracture surface of the PC bracket. A 30 um amorphous layer of

Figure 29: SEM Photograph of the Sapphire Bracket Fracture Surface

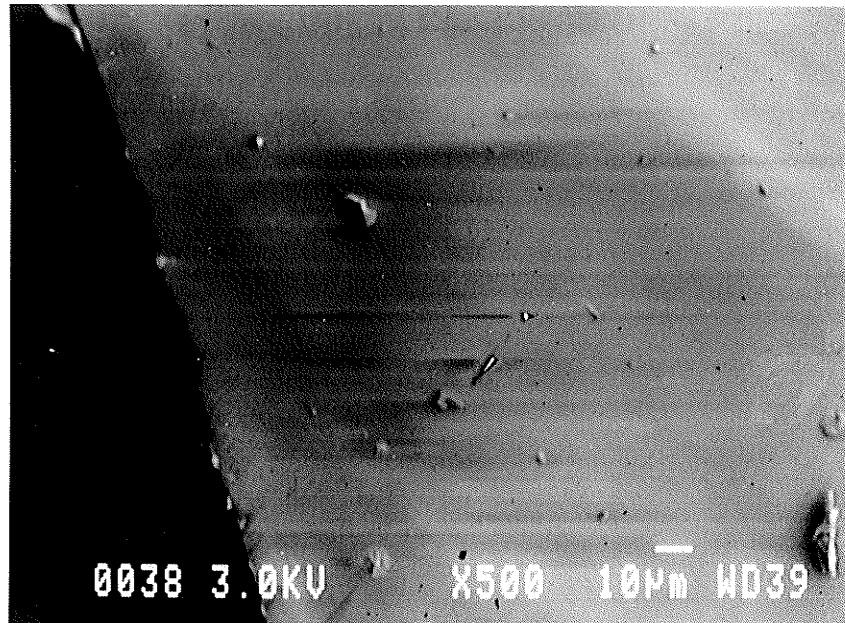
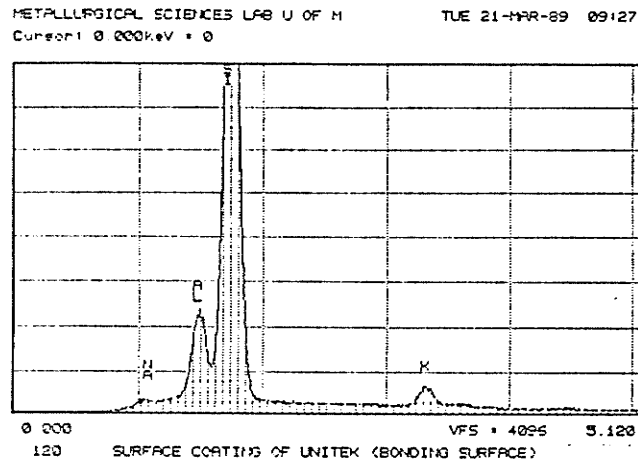


Figure 30: SEM Photograph of the Polycrystalline Bracket Fracture Surface. Note 30 um 'amorphous' layer at bonding surface interface.



material fused to the bonding surface of this bracket can also be seen. Analysis of this layer, Figure 31, revealed a composition similar to glass with Si, NA, and K predominating.

Figure 31



### Laser Debonding

Laser parameters were initially set at 5 watts, 44 Hz and 37 Kv with a 10 ns pulse width at 248 nm (KrF). Four samples were tested with the 8 kg/cm<sup>2</sup> shear force applied. PC brackets were used to set the parameters because the sapphire brackets spontaneously blew off the tooth surface during irradiation and without any applied shear load. These findings were dramatically different than those seen in any of the pilot studies. Since the four PC brackets tested at 5 watts debonded in less than 2 seconds the power was dropped to 4 watts. The results for the PC brackets at 248 nm are listed in Table 2.

Table 2: PC bracket removal times (sec) using 248 nm KrF laser  
Laser Parameters: 4 w, 36.5 Kv, 49 Hz, 10ns pulse

1.	3.83	9.	0.34	
2.	3.67	10.	2.75	
3.	0.69	11.	2.26	
4.	3.30	12.	2.64	
5.	3.63	13.	3.85	
6.	0.50	14.	0.48	
7.	3.94	15.	2.00	
8.	0.50	Mean	3.09	SD 0.68
		(10 samples)		

Samples 3, 6, 8, and 9 were removed very quickly. These values were omitted in calculating the mean times for removal. The reasons for this omission will be discussed subsequently. An average lasing time of 3.1 seconds was required for the removal of the PC brackets at this wavelength under these parameters.

The results obtained for the S brackets are in Table 3.

Table 3: S brackets removal times using 248 nm KrF laser  
Laser parameters: 4 w, 36.5 Kv, 49 Hz, 10 ns pulse

1.	0.30	+SF	9.	0.20	-SF
2.	0.29	"	10.	0.15	-SF
3.	0.42	"	11.	0.19	2.5w -SF
4.	0.17	"	12.	0.38	1.5w -SF
5.	0.22	"	13.	0.21	0.75w-SF
6.	0.15	-SF	14.	0.20	0.4w -SF
7.	0.17	-SF	15.	0.00	0.33w-SF
8.	0.17	-SF			

SF = shear force

Bracket removal times were very short, within the range of timing error calculated (Appendix 4). After the first 5 samples were debonded the shear force was removed. The next 5 samples, tested without a shear force, also gave extremely low removal

times. Thus the next 5 samples were removed with diminishing laser output power. The times for bracket removal continued to be well within the timing error measured to be  $0.31 \text{ sec} \pm 0.15$  seconds. It is possible that bracket removal could be achieved in a single pulse, but this could not be measured. The wattage was reduced by reducing the frequency from 29 Hz in sample 11 to 1 Hz in sample 15. As the samples were irradiated a crackling sound was heard as almost instantly the bracket blew forward off the tooth surface.

At 193 nm (ArF) only a limited number of samples were tested. The maximum power obtained from the laser was 1 watt at 118 Hz and 39.9 Kv. Debonding times for PC and S brackets tested are listed in Table 4.

Table 4: S and PC bracket removal times using 193 nm ArF laser  
Laser parameters: 118 Hz, 39.9 Kv, 1 w, 10 ns pulse

Polycrystalline		Sapphire	
1.	26 s	1.	1.02 min
2.	44 s	2.	> 1.30 min
3.	16 s	3.	> 1.30 min
4.	53 s	4.	> 1.30 min
<u>5.</u>	<u>38 s</u>	<u>5.</u>	<u>&gt; 1.30 min</u>
Mean	35 SD 15s	Mean	> 1.30 min

Note that only one S bracket was debonded. All other brackets were irradiated for 1.5 minutes without debonding.

At 308 nm (XeCl) 4 watts of power was obtained with 35 Kv and 36 Hz. The results are shown below in Table 5.

Table 5: PC bracket removal times (sec.) using 308 nm XeCl laser  
Laser parameters: 4 w, 36 Hz, 35 Kv, 10 ns pulse

1.	5.86	9.	5.06
2.	4.85	10.	3.93
3.	5.35	11.	4.69
4.	4.33	12.	0.70
5.	0.84	13.	4.16
6.	4.16	14.	4.57
7.	4.53	15.	5.64
8.	0.93	Mean	4.76 SD 0.6
			(12 samples)

Again several samples, numbers 5, 8, and 12, gave extremely low values. These were omitted when calculating the mean. The results at 308 nm for the S brackets were very similar to those obtained at 248 nm, Table 6.

Table 6: S bracket removal times (sec.) using 308 nm XeCl laser  
Laser parameters: 4 w, 36 Hz, 35 Kv, 10 ns pulse

1.	0.50	+SF	9.	0.19	-SF
2.	0.36	"	10.	0.31	-SF
3.	0.36	"	11.	0.20	2.7w -SF
4.	0.28	"	12.	0.30	2.1w -SF
5.	0.38	"	13.	0.85	1.1w -SF
6.	0.22	-SF	14.	0.92	0.6w -SF
7.	0.25	-SF	15.	8.14*	0.15w-SF
8.	0.21	-SF			

\* see text for explanation

The initial five samples were tested with the shear force applied. Five more were treated without applying the shear force. Debonding times were again very short. The remaining 5 samples were tested with decreasing laser output energy. Note that the energy output was modified by adjusting the frequency, from 26 Hz in sample 10 to 1 Hz in sample 15. Sample 15\* appeared to take much longer to debond, however, on closer inspection the bracket had been debonded but was still hanging in place.

Polycrystalline brackets were also removed with the 1060 nm Nd:YAG laser operating at 4 watts, 9 ns pulse width (Q-Switched) and at 17 Hz., Table 7.

Table 7: PC bracket removal times using 1060 nm Nd:YAG laser  
Laser parameters: 4 w, 17 Hz, 9 ns pulse (Q-switched)

1.	21.04	9.	23.56
2.	1.33	10.	32.06
3.	0.62	11.	12.52
4.	3.13	12.	35.19
5.	21.92	13.	19.78
6.	4.59	14.	7.83
7.	12.44	15.	<u>38.95</u>
8.	19.32	Mean	23.68 SD 9.01
			(10 samples)

Several values, 2, 3, 4, 6, 14 were felt to be low enough as to represent a secondary or altered population as has been identified with the two previous wavelengths tested.

The results obtained with 1060 nm debonding of the sapphire brackets continued the trend seen with 248 and 308 nm. Seven brackets with or without the applied load were removed rapidly at 4 watts power. The remaining 8 brackets were tested at varying power values as seen in Table 8.

Table 8: S bracket removal times (sec.) using 1060 nm laser  
Laser parameters: 4 w, 17 Hz, 9 ns pulse(Q-switched)

1.	0.48	+SF	8.	0.50	3.8w -SF
2.	0.66	"	9.	0.44	3.2w -SF
3.	0.84	"	10.	7.0 s	2.7w -SF
4.	0.50	"	11.	>1 min	2.5w -SF
5.	0.53	"	12.	>1 min	2.5w +SF
6.	0.50	-SF	13.	0.56	2.7w +SF
7.	0.50	-SF	14.	8.0 s	2.7w -SF
			15.	1.30	3.2w -SF

The power output of the Nd:YAG laser was altered in a different manner than that of the excimer wavelengths. Rather than changing the frequency, the laser energy was decreased by decreasing the voltage of the flashlamp. This decrease of voltage had a direct effect on the energy\pulse. It appears that with or without the force applied, greater than 1 minute would be required to remove the bracket at 2.5 watts. This wattage corresponds to a pulse energy of 147 millijoules. At 2.7 watts debonding time varied with the application of a shear force. If the force was applied the bracket was removed quickly. If it was not, 7 or 8 seconds was required for bracket removal. This wattage corresponds to a pulse energy of 159 millijoules. For all wattages above this value all brackets blew off instantly.

Statistical analyses (T tests) show significant differences exist between the debonding time of the sapphire and polycrystalline brackets ( $p < .001$ ), and between the various wavelengths used for the PC brackets ( $p < 0.001$ ). Tests were not performed between the various sapphire results because debonding times were so low, and within timing error. Note that a number of samples were eliminated when calculating the mean removal times. These brackets gave unusually low debonding times and were felt to represent an altered population of brackets. It has been reported that silane on the bonding surface of the brackets can be depleted by heat, light and moisture<sup>65,120</sup> resulting in weaker bond strengths. The brackets obtained from Unitek were samples retrieved from various clinicians for conversion into



Transcend 2000 brackets. They did not come from the same batch number and were probably stored under variable conditions.

In order to eliminate the possibility of artificially creating significant results by elimination of some data, a non-powermetric statistical analysis was performed. The Krushal-Wallis test is based on a Median number for each group. All 45 samples (PC) were used. Results showed significant differences between all groups, similar to the results of the T tests.

#### Damage Evaluation

Inspection of all debonded samples with the Zeiss binocular microscope up to 40x power revealed no apparent damage to the enamel surface or bracket. The raw data characterizing each bracket failure is found in Appendix 4. The bracket-adhesive (B\A) interface dominated the site of fracture for all the PC brackets tested. While some samples (10 of 45) showed less than 10% of total surface area of enamel-adhesive (E\A) fracture only 4 of these brackets showed any appreciable E\A fracture. Three of these, samples 2, 3, 4 at 1060nm irradiation had what appeared to be very short debonding times and were considered part of the altered population of brackets. Some brackets appeared to have carbon deposits associated with the debonded surfaces. A lower incidence of carbonization was observed with the 1060 nm brackets.

The results obtained with the sapphire brackets differed substantially from those seen in previous pilot studies. Seven brackets at 248 nm exhibited complete B\A failure. All others

tested, except one at 308 nm, displayed complex failure patterns. Greater than 50 % of the bracket base area failure occurred at the B\A interface, yet all brackets demonstrated some degree of E\A or intra-adhesive (I\A) failure. A representative number of samples, 5 of each bracket type at each wavelength, were examined under SEM. Figure 32 shows the typical 'complex' debonding pattern found with the Sapphire brackets. Figure 33 is a close up of Figure 32 which demonstrates the bracket\adhesive fracture on the left, with a wall of adhesive that ends at the enamel/adhesive interface. At 500x magnification, Figure 34, the enamel rod morphology is more evident. This enamel does not however, appear similar to etched enamel. No apparent enamel damage was seen under SEM.

Figure 35 illustrates the typical appearance of the bracket/adhesive site of failure found with the PC brackets. A closer view, Figure 36, of the light area within the debonded resin face, in Fig. 35, demonstrates an unusual pattern of smooth walled clefts or bubbles. Again no apparent enamel damage could be found.

Figure 32 : SEM photograph of complex debonding pattern common to sapphire bracket samples, (15x magnification)

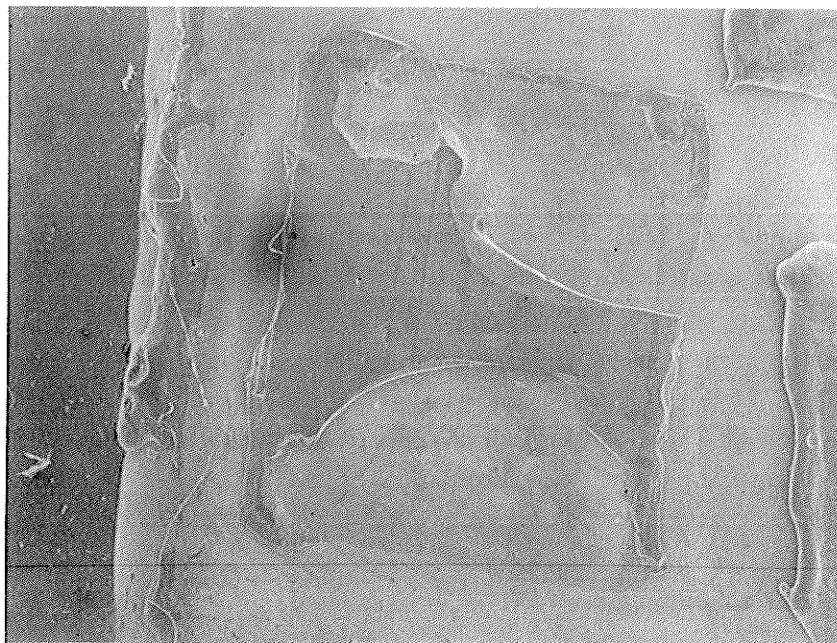


Figure 33 : SEM photograph (200x) demonstrating both bracket/adhesive (left) and enamel/adhesive interface fracture sites.

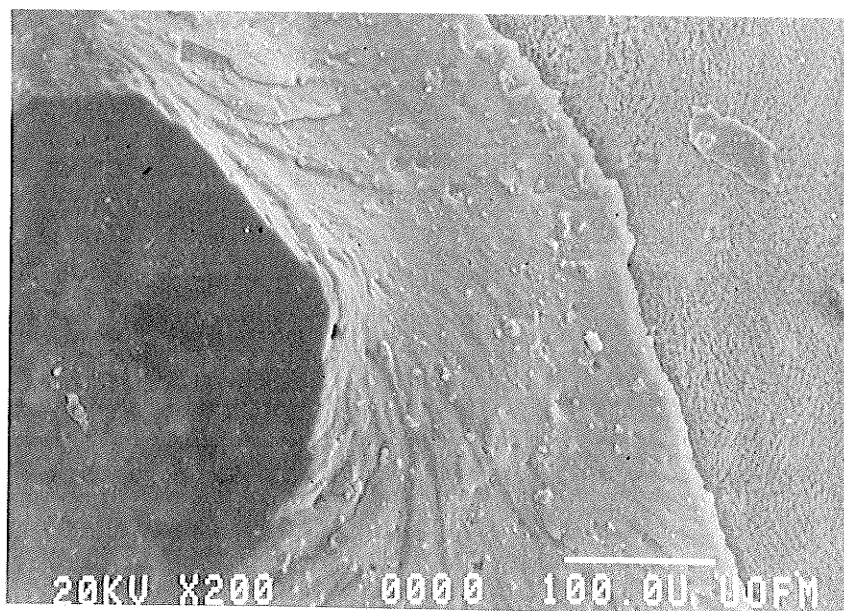


Figure 34 : SEM photograph (500x) demonstrating enamel appearance adjacent to resin wall.

